# An Automatic Profiler of the Temperature, Wind and Humidity in the Troposphere

D. C. HOGG, M. T. DECKER, F. O. GUIRAUD, K. B. EARNSHAW, D. A. MERRITT, K. P. MORAN, W. B. SWEEZY, R. G. STRAUCH, E. R. WESTWATER AND C. G. LITTLE

*NOAA/ERL/Wave Propagation Laboratory, Boulder, CO 80303*

(Manuscript received 13 September 1982, in final form 6 December 1982)

ABSTRACT

A remote-sensing system for continuously profiling the troposphere is discussed; the prototype Profiler utilizes radio wavelengths, thereby achieving essentially all-weather operation. Designed for unattended operation, the Profiler employs radiometric and Doppler radar technology. Design, construction and calibration of the instruments composing the Profiler system are described along with some of the physics and mathematics upon which their operation is based. Examples of profiles and other variables of meteorological interest are given, and comparisons are made with simultaneous data from colocated operational (NWS) sondes. An algorithm based on climatological statistics of measurements by radiosonde is used in the radiometric retrieval process, but there is no reliance of the products of the Profiler upon any current radiosonde data. The role of the Profiler in mesoscale and synoptic weather forecasting and its relationship to systems employing sounders on satellite platforms are also discussed.

## 1. Introduction

There is a move afoot within the various services that provide measurements of the temperature, wind, and humidity in the troposphere toward automated instrumentation, and questions justifiably arise regarding the reliability, accuracy, and complexity of the automated instruments. It is desirable that the new instruments provide additional measuring capabilities that may be beneficial to weather forecasting. For the Profiler system discussed here, perhaps the most significant new feature is continuity in time in measurement of profiles and integrated quantities such as total precipitable water vapor. This capability is especially pertinent to mesoscale meteorology where knowledge of atmospheric changes that occur more rapidly than those resolved by twice-daily radiosondes is important. Examples of these rather rapid temporal changes in the temperature, wind, and humidity are given in the following sections.

Regarding reliability, there are two factors: reliability in the sense of low maintenance on the hardware and software of the instrument, and reliability in accurate measurement of the atmospheric variables during all weather conditions. The former is addressed by designing the Profiler using primarily solid-state technology, and by requiring that there be no moving mechanical parts in the system. The requirement for operation during almost all weather conditions is addressed by utilizing remote-sensing instruments that operate at radio wavelengths. Since clouds, fog, snow, and light rain are semi-transparent to these waves, reliable measurements are obtained almost all the time.

The question of economics is addressed in part by designing the Profiler for unattended operation; manpower requirements are therefore minimized. The Profiler utilizes both passive (radiometric) and active (radar) remote sensors. Experience over more than two years has shown that the radiometric sensors can indeed be relied upon in unattended operation; the component requiring most attention has been an associated computer. The Doppler radars in the prototype Profiler (for measurement of wind, and intensity profiles of back-scattered signals) are of two types—one operating at VHF, the other in the UHF band. The former, although operated continuously, was initially built for experimental purposes, and not designed for high reliability; the latter is solid-state throughout and is designed to require little attention over the years. It is estimated that the capital cost of a Profiler designed for unattended operational use would be defrayed in about seven years, when compared with the costs of labor and expendibles incurred by a radiosonde station launching two units per day. The surface instrumentation used with the Profiler has been found by experience to be least reliable, the surface humidity sensors being particularly troublesome.

The questions of accuracy and complexity are discussed in the body of the text. Briefly, it is found that the Profiler measurements of total precipitable water vapor, and wind measurements, are believed more accurate than obtained by conventional radiosonde and rawinsonde. Profiler measurement of the 500 mb pressure height is at least as accurate as radiosonde. Vertical winds and zenith-integrated cloud liquid, two variables not routinely measured by sonde, are believed accurate to about 0.1 m $s^{-1}$ and 0.1 mm respectively. However, the Profiler measurements of temperature and humidity profiles do not, at present, faithfully reproduce inversions that have sharp gradients. This behavior, which exists because passive radiometric instruments are integrating devices, can be remedied considerably by use of additional information from active sensors such as radars and ceilometers. For this reason the Profiler is referred to as a system; information from one sensor complements the performance of another. This joint profiling method is discussed in some detail in Section 7, along with examples of measured data.

## 2. Radiosondes of the present upper-air system

The standard for comparison of new instruments measuring the behavior of the upper air, is the radiosonde. It is therefore worthwhile to address briefly the nature and accuracy of the reference used in evaluating Profiler measurements.

In both time and space, radiosonde and rawinsonde measurements differ significantly from those of the Profiler. Radiosondes are launched twice daily by the National Weather Service (NWS) of the United States. Point measurements are taken according to the rules set forth in the Federal Meteorological Handbook No. 3, *Radiosonde Observations*. The measurements are taken at instants in time so it is not possible to compute a time average of some variable (for example wind at a given altitude) over some desired interval of time (e.g., an hour). The radiosonde takes about half an hour in ascent to tropopause altitude; thus since conditions are usually changing with time, "snapshot" profiles may not be obtained. Spatially, the balloon may drift many tens of kilometers from the zenith of the launch site whereas the Profiler is fix-pointed in the vertical; this often makes meaningful comparisons of rawinsonde and Profiler data at high altitudes difficult.

A study (Hoehne, 1980) of the relative precision of rawinsondes was recently undertaken at the Test and Evaluation Division of NWS. Two electronic packages were launched on a single balloon, one the operational sonde for Washington, D.C., and the second, a "test" sonde which utilized a different telemetering frequency (and therefore a different tracker) than the operational sonde. The sondes had the same temporal resolution. Fifty weekly sonde-pair flights were made during a year. This type of comparison provides the *functional precision* (relative readings for a given variable, say temperature) of the two sonde packages; it is not a measure of absolute accuracy. The numbers that result can, however, be considered representative of the maximum accuracies to be expected using operational sondes. A bias in temperature and humidity is caused in part by the heat of the upper package affecting the lower package.

Table 1 shows the results obtained in the comparison when data for the two sondes at the same pressure heights are used; the "upper" sonde is the test package, and the "lower" sonde the operational package. In all cases, the rms for the relative precision was found to be closely equal to the standard deviation of a fitted Gaussian. These functional precisions will be referred to in the Profiler–sonde comparisons that follow, recognizing that they are the only published computations of precision of operational sondes known to us.

There are bases other than accuracy upon which comparisons between sondes and the Profiler can be made, for example timeliness of forecasts. Since synoptic models are updated from radiosonde data obtained at specific times, as mandated by worldwide agreement, the forecasts are not optimal with respect to local time. With continuous profiling, the updating could be done at times most suitable for producing the best and most timely forecast for the public living at a given location.

## 3. Profiler design

Several criteria govern the design (Hogg *et al.*, 1980a) of the Profiler system. These requirements include: operation during essentially all weather conditions, including snow, fog, cloud and light rain; unattended operation; high reliability; and conservative design in the data system.

Within the constraints of those criteria, several associated conclusions are reached; these include: use of radio wavelengths; fully automatic operation necessary; remote sensors must have no mechanical moving parts, e.g., fixed multiple beams are required for the antenna of the wind-profiling Doppler radar; solid-state electronics should be used; error correction must be incorporated in the data system.

A block diagram of the prototype Profiler is shown in Fig. 1; the following subsystems are included: a six-channel temperature/humidity profiling radiometer, two operating near 20 and 30 GHz, and four between 50 and 60 GHz; instruments for surface measurements, including pressure, temperature, hu-

TABLE 1. Functional precision of NWS radiosondes; data apply to two sondes at the same calculated pressure height (see Hoehne, 1980); data taken at Sterling, VA, near Washington, DC.

| | Temperature (°C) | Dew-point depression (°C) | Precipitable water vapor (mm) | Wind vector (m $s^{-1}$) | Pressure (mb) |
|---|---|---|---|---|---|
| Bias upper − lower sonde | −0.19 | +0.38 | −0.53 | 0.0 | −0.1 |
| Root mean square | ±0.86 | ±3.44 | ±1.39 | ±3.1 | ±0.7 |

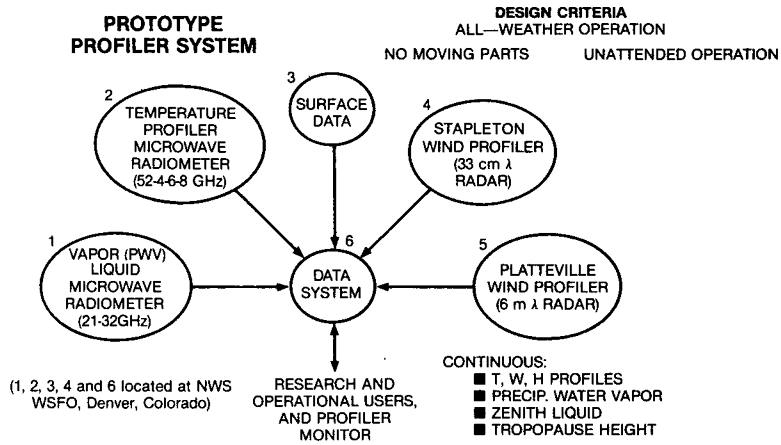


FIG. 1. Subsystems of the Profiler located near the NWS WSFO, Stapleton Airport, Denver, Colorado; 1 and 2 are passive (radiometric) remote sensors; 4 and 5 are active (Doppler radar).

midity, wind, and rain rate; wind-profiling Doppler radar, one operating in the VHF (50 MHz), the other in the UHF (915 MHz); data system, including a host computer that provides an accessible data base, and auto-dial equipment.

The details of these subsystems, their interacting roles, and the techniques of profile retrieval from the remotely sensed data are discussed in the following sections. Although design of the instruments is emphasized, typical examples of measured data are also presented. Note that integrated liquid water in the vertical direction, a measurement not provided by radiosonde, is available from the Profiler. A companion paper in this issue (Hogg *et al.*, 1983) contains discussion of the design and implementation of a related instrument, a steerable-beam radiometer with 20- and 30-GHz channels; this is used in research on water vapor, and on supercooled liquid in clouds.

The building for housing much of the electronics of the Profiler (Fig. 2), is located on the same property as the Weather Service Forecasting Office (WSFO), Stapleton Airport, Denver, Colorado; the radiosonde launch site is also located there. There were several reasons for choosing this location, the most significant being that comparisons can be made routinely with twice-daily NWS radiosondes. It was also rec-

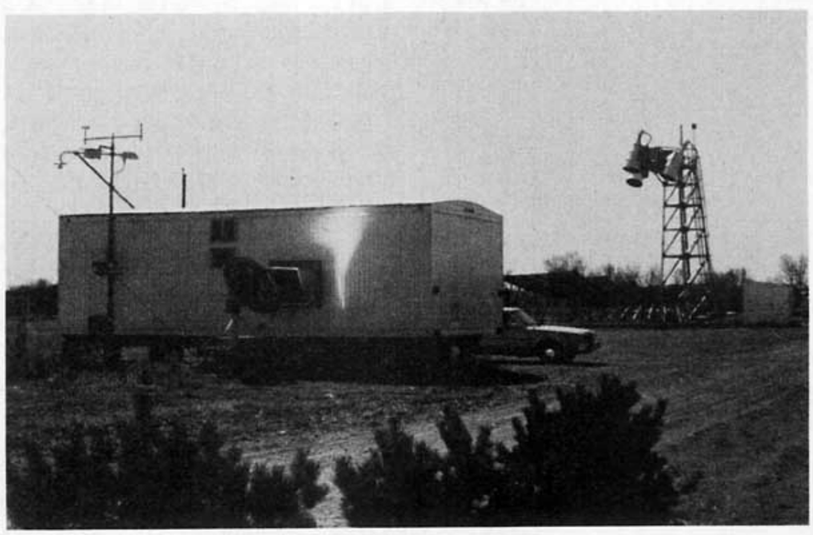

FIG. 2. The Profiler building near the NWS WSFO at Denver. Note the flat 45° millimeter-wave reflector and canopied window of the radiometric antenna; on the right is the triple-beam UHF antenna and transmitter building; the Profiler building houses the radiometers, UHF radar receiver, the host computer and peripherals, and some of the surface instruments. The flat ground just visible on the far left is the launching area for NWS radiosondes.

ognized that the adequacy of the Profiler could be tested by long-term comparison with the sondes, and that cooperation with the operational forecasters would be fostered (see, e.g., Hogg *et al.*, 1980b). It must be emphasized, however, that real-time upper-air measurements provided by the Profiler are completely independent of any current radiosonde data.

The VHF wind-profiling radar is located at Platteville, Colorado, about 50 km north of Denver. This instrument was designed and built by the Aeronomy Laboratory of ERL, NOAA, for research purposes (see e.g., Gage and Balsley, 1978). Antenna beams of width 3.5° pointed 15° from vertical, to the north and east, allow measurement of high-altitude horizontal winds routinely (Section 6a); these data are auto-dialed by the host computer (Section 8) at the WSFO, Denver, for transmittal to the users. Vertical winds and tropopause heights are measured by a separate VHF antenna that generates a vertically pointing beam.

## 4. Surface measurements

A commercial microprocessor-based data-logging system (Campbell Instruments, model CR121) is used in measurement of the surface temperature, relative humidity, pressure, wind speed, wind direction, and rain rate. Sensors for pressure and rain rate have been added to the CR121. It has an assortment of internal programs that control not only the timing of the sampling of the sensors but also scaling of their outputs to the required engineering units. There are programs that take averages, keep track of minimum or maximum values within a specified time, and transmit the requested values to other devices via a standard RS232 serial interface. Our unit operates with a basic sampling period of 2 minutes. Ten 2-minute samples are averaged and transmitted to the Profiler host computer (see Section 8) as well as to a teletype terminal for display. The 20-minute averaging is for display; it is not mandated by host-computer considerations. Table 2 lists the accuracies specified by the manufacturer for the sensors, including the effect of linearization of scaling by the CR121.

TABLE 2. Surface instrumentation and accuracies.

| Sensor | Type | Range | Accuracy |
|---|---|---|---|
| Temperature | Thermistor | −20 to +35°C | ±0.4°C |
| Relative humidity | Hygristor | 10 to 97% | ±3% |
| Wind speed | Cup anemometer | | 0.25 mph or ±1.5% |
| Wind direction | Vane | 0 to 360° | ±5° |
| Pressure | Aneroid | ±50 mb | ±0.5 mb |
| Rain rate | Tipping bucket | 0–200 mm h$^{-1}$ | > ±0.5% |

TABLE 3. Center frequencies for channels used in the radiometric system.

| Channel | Frequency | Atmospheric constituent most effective | Bandwidth (GHz) |
|---|---|---|---|
| 1 | 20.60 | water vapor | 1.0 |
| 2 | 31.65 | liquid | 1.0 |
| 3 | 52.85 | temperature | 0.1 |
| 4 | 53.85 | temperature | 0.1 |
| 5 | 55.45 | temperature | 0.1 |
| 6 | 58.80 | temperature | 0.1 |

The surface measurements of temperature, humidity and pressure are incorporated in retrieval of the temperature and humidity profiles (see Section 5). The surface wind information is for use as the initial data point for the wind profiles (see Section 6b). The rain rate is used primarily for correlation with the zenith-integrated liquid measured by the radiometers (see Section 5).

## 5. Microwave radiometers for measurement of temperature, vapor, and liquid

### *a. Selection of frequencies*

Choice of microwave frequencies appropriate for remotely sensing the temperature and humidity is governed by the wavelengths of oxygen and water vapor absorption lines. Oxygen absorbs over a band of frequencies from roughly 50 to 70 GHz, and also at 118 GHz, whereas water vapor has absorption lines near 22 and 183 GHz. Absorption by liquid water, on the other hand, increases monotonically with frequency over the entire microwave band (Hogg and Chu, 1975). Since a large amount of liquid (i.e., rain), limits the capability of radiometers, it is preferable, for all-weather operation, to utilize the lowest microwave frequencies possible. In the prototype Profiler, a frequency near 22 GHz is used primarily for vapor, and the 50–60 GHz band for temperature. Oxygen, with its constant mixing ratio, is an ideal gas for radiometric measurement of temperature. A frequency near 30 GHz, well removed from the oxygen and vapor absorption lines, is used primarily for measurement of zenith-integrated liquid. Ice particles and dry snow have negligible absorption, and therefore produce no effect on the microwave radiometers. Table 3 shows the center frequencies for each of the six channels used in the radiometric system.

The frequency primarily for vapor measurement is 20.6 GHz rather than 22.2 GHz which is the frequency of the peak of the absorption line. This off-line-center choice is made because the derived total amount of vapor is then relatively independent of the pressure (i.e., height) of the vapor (Westwater, 1967).

The combination of 20.6 and 31.65 GHz constitutes a dual-channel radiometer that is useful in weather modification and other special research programs as discussed by Hogg *et al.,* 1983.

The four channels 52.85 through 58.80 GHz are located on the low-frequency side of the oxygen absorption band. The lowest absorption of these therefore occurs at 52.85 GHz, and emission from the entire troposphere is sensed effectively by this channel. On the other hand, 58.80 GHz is a highly absorbing channel, and significant emission is received from only the lowest kilometer of the troposphere. The 53.85 and 55.45 GHz channels, which absorb at strengths intermediate between the other two, are sensitive mainly to the oxygen up to mid-altitudes (e.g., 2 to 6 km above the surface). By combination of the emission in all of these channels, profiling is achieved as discussed in Section 5d.

### b. *Six-channel radiometer for temperature/humidity profiling*

All six radiometers are of similar design, but the bandwidths of the channels differ, as indicated in Table 3. The channels used for temperature sensing utilize a relatively narrow bandwidth (0.1 GHz) to provide sufficient discrimination between channels.

The antenna beams for all channels point to zenith, and have essentially the same shape and beamwidth. The latter is an important feature in properly accounting for liquid-bearing clouds that pass through the beams. If the beamwidths were unequal, a liquid-bearing cloud entering the system would produce a "signal" in some channels, and none in the others, and correction of the retrieved temperature and humidity for the emission by the liquid in the cloud would not be feasible. The antennas for all channels are offset paraboloids located inside the Profiler building. Emission from the zenith is reflected by the 45° flat reflector, shown in the photograph (Fig. 2), through a microwave window protected by a cowling, to the paraboloids where it is focused into the radiometers. Each of the three paraboloids accommodates two channels. The 45° flat reflector is scannable in elevation angle for calibration purposes.

A block diagram of the electronics for a channel is shown in Fig. 3. Emission from the atmosphere incident on the antenna is shown by dashed lines; the energy is guided to a terminal of a three-way microwave switch, the heart of the radiometer (Guiraud *et al.,* 1979). The common arm of the switch feeds the mixer, and amplifiers which determine the bandwidths referred to in Table 3. On the other two terminals are reference loads at different, highly regulated temperatures. As the switching sequence progresses the power from these two loads is fed

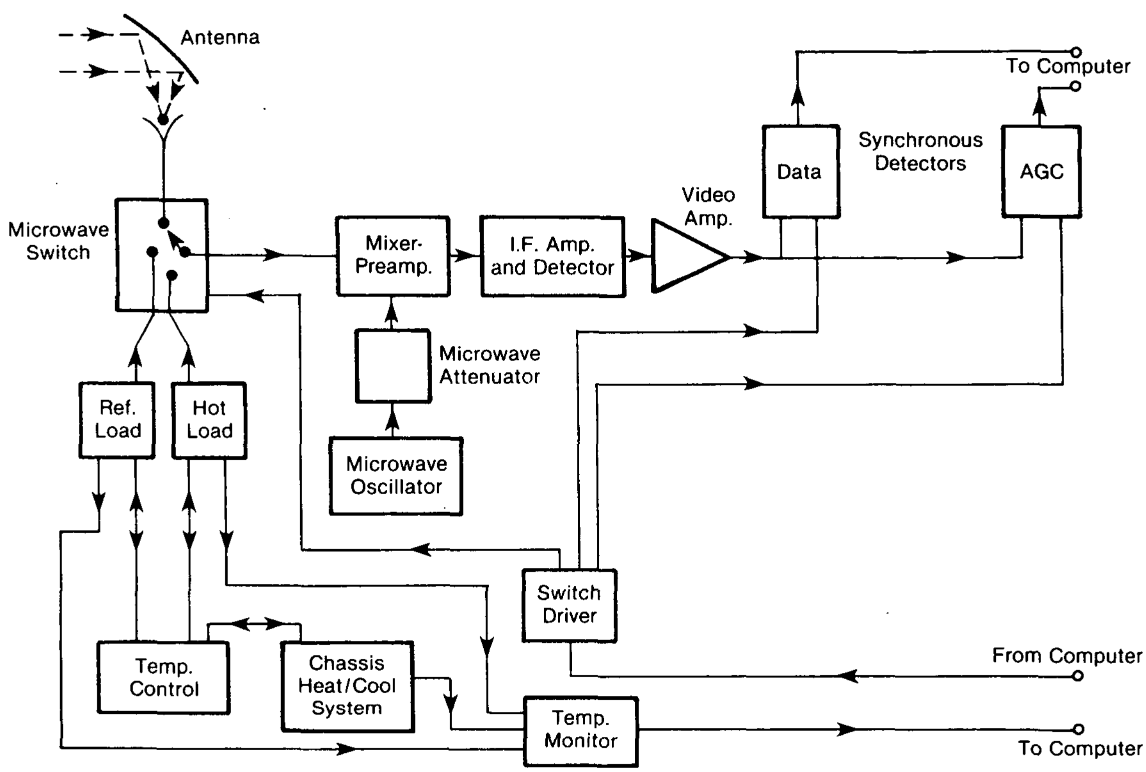


FIG. 3. Components of a radiometer.

sequentially through a synchronous detector which is gated by the driver. A voltage that represents the state of the amplifiers is thereby provided to the computer for correction of changes in gain (AGC). It is this feature that provides high stability in the radiometer; i.e., the radiometer is continuously self-calibrating. The voltage generated by the radiation from the atmosphere incident on the antenna (the "signal") proceeds in a similar manner to the computer.

*c. Calibration procedure*

The basic measurement provided by each channel is a "noise temperature" that represents the power within the channel bandwidth. Referring again to Fig. 3, if the switch is on the hot load terminal for example, the noise temperature indicated by the radiometer is the actual temperature of the load, provided there are no power losses in the connecting microwave waveguides. However, small losses do exist and must be accounted for in the calibration.

Losses in the antenna, connecting waveguides, switches, etc., attenuate the desired signal and contribute their own radiation to modify the observation of the atmospheric radiation. These losses, which are essentially constant, may be measured by observing a range of known radiation (brightness temperatures) with the complete system. At 20.6 and 31.65 GHz, the atmospheric brightness temperatures under clear sky conditions (horizontal homogeneity) are determined by scanning the antenna beam in elevation. The losses are then determined directly by this procedure as discussed by Hogg *et al.*, 1983. At the frequencies of the four temperature-sensing channels, knowledge of the actual physical temperature of the atmosphere becomes essential for calibration because the elevation scan procedure is inaccurate. Known brightness temperatures for these frequencies are obtained from 1) a matched microwave absorber at a known temperature, and 2) atmospheric brightness temperatures computed from radiosonde data. Other accurate calibration methods, independent of the radiosonde, are under investigation.

*d. Profile-retrieval method*

The brightness temperatures from the six-channel radiometer, along with surface measurements of pressure, temperature, and humidity, constitute nine known pieces of information that are used for retrieval of the profiles. The method, called linear statistical inversion (Westwater, 1972), is based upon techniques developed by Wiener (1949) and Kolmogorov (1941). The inversion algorithm for temperature retrieval, can be written

$$\hat{T}(h) = c_0(h) + \sum_{i=1}^{9} c_i(h)x_i,$$

where $\hat{T}(h)$ is the estimated temperature at altitude $h$, and the $x_i$ are the nine observed values (or related variables) discussed above. The $c$'s are the all-important retrieval coefficients; these are calculated using the radiative transfer properties of the atmosphere and *a priori* radiosonde data for a several-year period, for given climatologies. The absorption coefficients of oxygen and water vapor determine the radiative transfer at the microwave frequencies of interest (Table 3); these are known to good accuracy. A detailed discussion of statistical inversion as applied to microwave temperature/humidity profiling is given by Westwater (1972).

*e. Examples of radiometrically measured data*

Previous experience with measurements by ground-based microwave radiometric profilers (Decker *et al.*, 1978) showed that the rms differences in temperature and humidity, obtained by comparing radiometric data with radiosondes, are predictable. Calculation of these differences involves the noise level of the radiometric instrument and the effectiveness of the algorithm that corrects for the presence of liquid-bearing clouds. The differences can be computed for the profiles or for derived (integrated) quantities such as pressure heights and pressure-layer thickness. Since the Denver Profiler is designed for high stability, and since radiometers are integrating instruments, measurements of such derived quantities have been shown to have accuracies competitive with those of radiosondes.

The measurement of zenith-integrated values of vapor [the total precipitable water vapor (PWV)] is discussed in detail by Hogg *et al.*, (1983). Briefly, the PWV is measured to an rms accuracy better than 1 mm (for PWV of about 1.5 cm) which is somewhat better than the precision of radiosonde data (see Table 1). The measurements of integrated liquid in clouds, are believed to be accurate to about 0.1 mm. A 3-day analog record showing the behavior of both integrated water vapor and liquid is given in the lower panel of Fig. 4. This example, one of many, is chosen because it demonstrates Profiler performance during both clear and unsettled weather conditions. As seen on the record of zenith-integrated liquid (the bottom plot in Fig. 4), the sky was devoid of liquid-bearing clouds on May 1. Following cloud buildup on May 2, about 5 mm of rain fell on May 3. The solid dots occurring every 12 h on the records are data from the NWS operational radiosondes at Denver.

Also shown in Fig. 4 are the time series of the heights of the 700, 500 and 300 mb pressure levels, again compared with radiosondes. It is interesting that rather steep decreases in the pressure levels, from 0600 to 2400 on 2 May 1981, preceded the high-liquid condition. It is clear, by comparison with accompanying radiosonde data plotted on the time se-

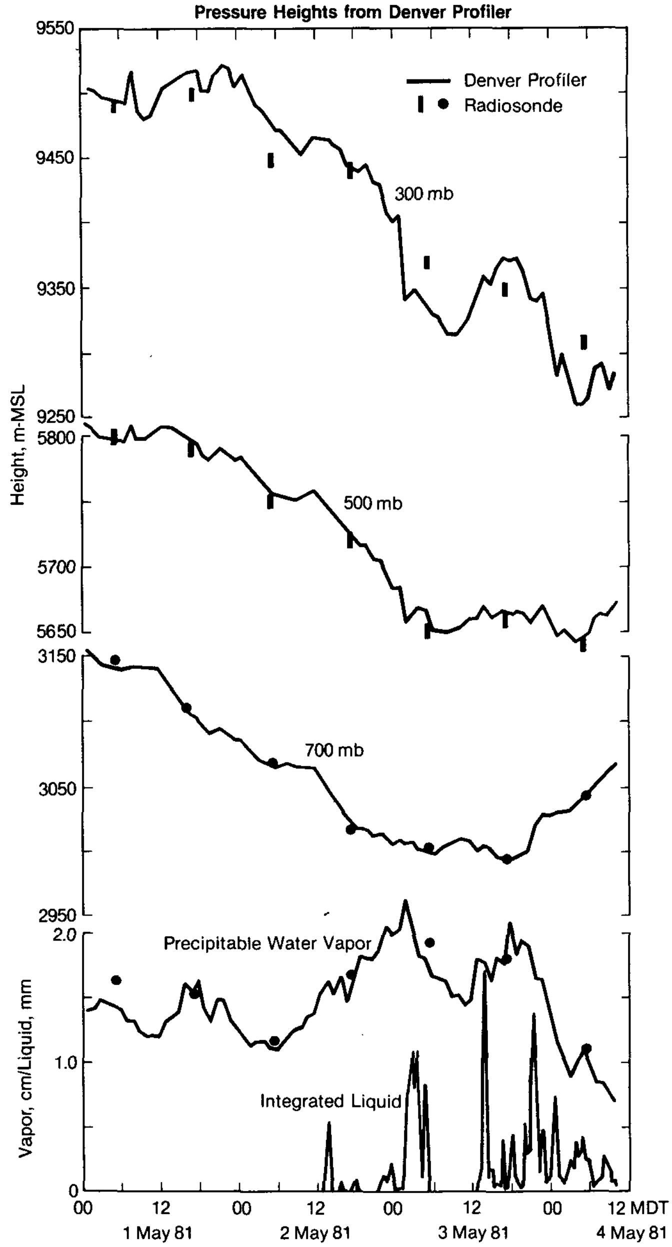


FIG. 4. Example of pressure heights, total precipitable water vapor, and integrated liquid in the zenith measured during clear conditions (1 May), and cloudy conditions with rain (2 and 3 May); the solid marks every 12 h are values obtained by Denver NWS radiosondes.

ries, that the Profiler/radiosonde differences are quite small for the 700 and 500 mb levels but are larger at the 300 mb level. This is partly because the Profiler radiometric measurements are less accurate at the higher altitudes, although some of the difference is due to the radiosonde whose accuracy also decreases with altitude. In Section 7, a technique of joint active/passive profiling is described; it improves considerably the radiometric profiles at the higher altitudes. Use of the technique will also improve accuracy of the heights of the 300-mb pressure level. Heights of the 0 and $-10$ degree isotherms are given in Fig. 5 for the same period.

Temperature profiles measured during the unsettled weather conditions of 3 May 1981 (see Fig. 4) are shown in Fig. 6. The profile measured by a radiosonde launched at 1700 MDT on May 3 is shown by a solid line in Fig. 6; at that time there was rela-

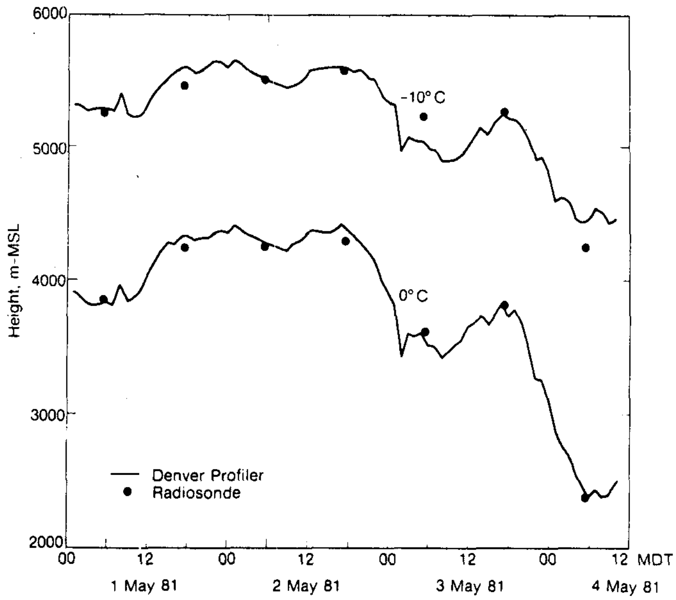


FIG. 5. Heights of 0° and −10°C isotherms for the same conditions as Fig. 4.

tively little liquid above the site as the lowest plot (liquid) in Fig. 4 indicates. The corresponding profile measured by the Profiler radiometers at 1700 MDT is shown by circles in Fig. 6; agreement between the two measurements is very good. At 1400 MDT a large amount of zenith-integrated liquid (1.7 mm) was present, as shown by the large peak in the lowest plot of Fig. 4. The profile measured by the radiometers for that time is shown by triangles in Fig. 6. Clearly the profile retrieved, even under this high liquid condition, is a good representation of the profile measured by radiosonde a few hours later.

Time series of profiles are useful in studies of air pollution. The strength and height of a capping in-

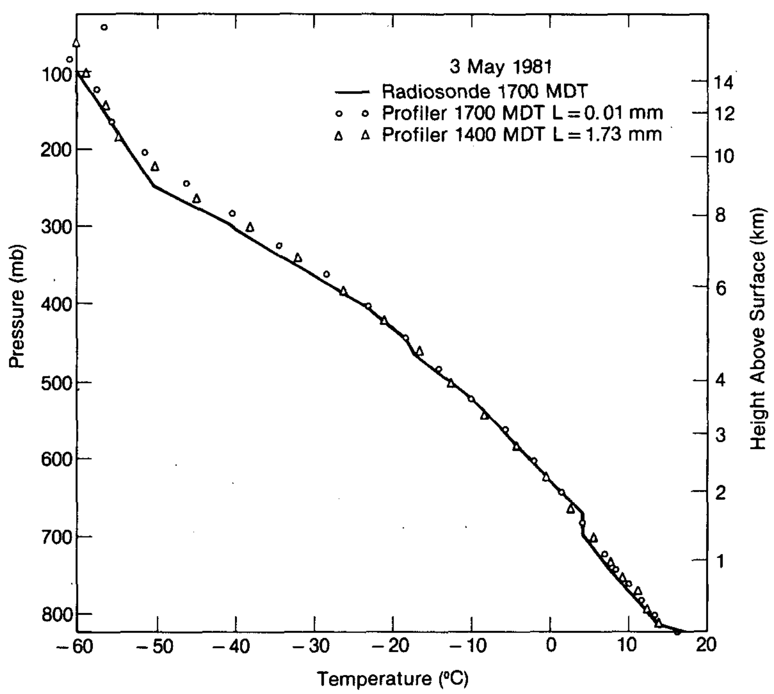


FIG. 6. Temperature profiles during the high liquid conditions of Fig. 4.

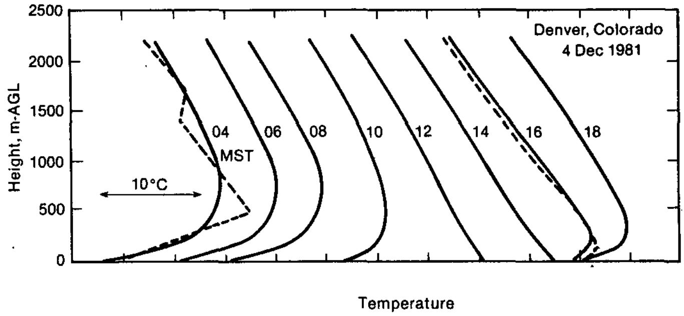


FIG. 7. Eight temperature profiles showing the behavior of a ground-based radiation inversion during a day with high air pollution at Denver; profiles are plotted every 2 h from 0400 to 1800 MST; successive profiles are displaced 5°C to the right of the preceding profile; dashed lines are profiles from the operational NWS radiosondes.

version, as a function of time, are helpful in gauging the persistence of pollution. Fig. 7 shows a set of eight profiles taken between 0400 and 1800 MST on 4 December 1981, a day with high air pollution at Denver. At 0400, the radiation inversion is strong, about 12 degrees, peaking at 700 m above ground. The strength decreases to about 4 degrees with a peak at an altitude of 300 m at 1000 MST. During noonday, the inversion disappears for a few hours, but re-forms by 1600 MST and strengthens; on this occasion, the time interval available for dispersion of the pollution was rather small. The Denver radiosondes for 0400 and 1600 MST are also shown; they provide more detailed structure than the Profiler, as expected. Improvement in resolution of radiometrically retrieved profiles using an active/passive method is discussed in Section 7.

*f. Adaptive retrieval of temperature profiles*

The accuracy of temperature and humidity profiles retrieved during conditions of low cloud liquid content $L$ ($L \leqslant 2$ mm) approaches the accuracy achieved during clear conditions. However, for heavy clouds ($L \geqslant 2$ mm) and for light rain (rain rate $\leqslant 5$ mm h$^{-1}$ originating at a height of 2 km), retrievals derived using statistical inversion (Section 5d) are degraded. An extension of the adaptive retrieval method of Westwater and Guiraud (1980) has shown promise in improving retrieval accuracy of profiles during high-liquid situations. In essence, retrieval coefficients that are a function of the amount of liquid $L$ are derived. The cloud liquid *per se* is accurately derived using nonadaptive methods, with the radiometric channels at 20 and 30 GHz (see Hogg *et al.*, 1983).

Fig. 8 shows a comparison of retrievals based on computer-simulated data using both the statistical and adaptive methods, for a high-liquid cloud ($L$ = 5 mm). Clearly the profile retrieved using the adaptive coefficients agrees with the radiosonde profile much better than does the profile retrieved using the constant (nonadaptive) statistical coefficients. This example and other computer simulations indicate that adaptive methods lead to substantial improvement in retrieval accuracy during conditions of high liquid. Implementation of this technique on the Profiler host computer system in real time is planned (see Section 8). If the adaptive coefficients are not used, the profile in the presence of heavy rain is too inaccurate (see Fig. 8) and is automatically discarded.

## 6. Radar for measurement of winds and inversion heights

*a. Principles of wind measurement*

Doppler radars for wind measurement require large apertures to achieve the sensitivity needed to detect scattering from refractive turbulence in the optically clear air (Gage and Balsley, 1978). Fixed-pointing antennas that avoid the costs and complexities of mechanically or electronically steerable an-

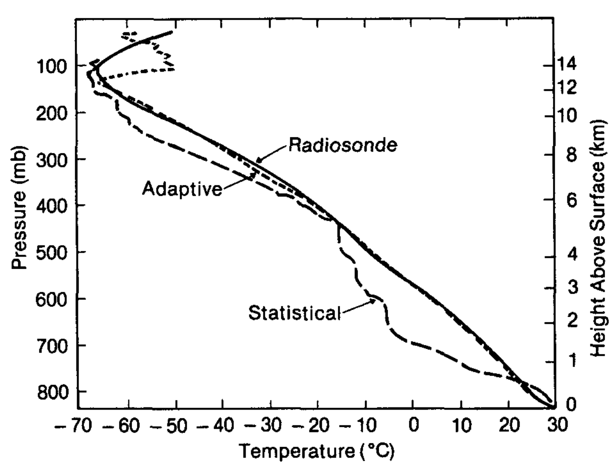


FIG. 8. Improvement in temperature profiling during conditions of high liquid achieved by use of adaptive retrieval coefficients.

tennas are suitable for measuring mean wind profiles. Three antenna beam-pointing directions are needed to measure the vector wind; for simplicity the pointing directions are chosen to observe orthogonal horizontal wind components and the vertical component. The horizontal wind must be measured using an elevation pointing angle ($\theta_e$) that allows observation at all altitudes of interest; the radar measures the projection of the horizontal and vertical winds onto the antenna pointing direction (i.e., the radial motion).

The radial Doppler velocities ($V_i$) measured by the radar are related to the wind ($u$, $v$, $w$) in an ($x$, $y$, $z$) coordinate system as follows:

$$\left.\begin{aligned} V_1 &= u\cos\theta_e + w\sin\theta_e \\ V_2 &= v\cos\theta_e + w\sin\theta_e \\ V_3 &= w \end{aligned}\right\},$$

where the antenna azimuth angles for $V_1$ and $V_2$ are assumed to be zero and 90° respectively. At each altitude $h$ the three measurements are made at volumes separated in space, so an assumption of horizontal uniformity is needed to combine the measurements to form a wind profile above the radar location. Two types of errors can result from this assumption: first, $u$ and $v$ measured at the observation volume will be in error by $h\Delta w/\Delta x$ and $h\Delta w/\Delta y$ respectively, and second, the measured $u$ and $v$ will differ from the $u$ and $v$ directly above the radar by $(\Delta u/\Delta x)h\cot\theta_e$ and $(\Delta v/\Delta y)h\cot\theta_e$ respectively.

The two radars used for the prototype Profiler (Strauch, 1981) operate at very different wavelengths (33 cm and 6 m); one is relatively sensitive to precipitation particles while the other is not, so data from the two radars are treated differently. The 6 m wavelength radar rarely observes precipitation, so the measured vertical velocities are directly related to vertical wind. Further, for long averaging times (20 min to 1 h), the vertical motions can usually be neglected in calculating the horizontal wind components. Thus, the primary purpose of the zenith-pointing antenna for the 6 m radar is not to measure $w$ but rather to measure the height of the tropopause (see Section 6e). On the other hand, the 33 cm radar (which is now undergoing initial test) readily detects scattering from hydrometeors which, at times, can be stronger than the scattering from refractive turbulence. Thus, this radar measures particle fall speed plus vertical wind ($w - v_t$) during precipitation, and the vertical motion of the particles must be used to correct the measured horizontal velocities; hydrometeor fall speed values can be as large as 9 m s$^{-1}$ (even larger for hail) (Atlas *et al.*, 1973). In the clear atmosphere the 33 cm radar can measure the vertical wind but during precipitation it cannot. For both radars, errors caused by horizontal gradients are minimized by using a high (75°) elevation angle for the antenna beam. It is obvious that if there are convective storms near the radar, significant errors in the horizontal wind measurement will result. However, in this case, a single Doppler radar, even with a fully steerable antenna, could not measure the wind profile; moreover, the actual wind profile would probably not be meaningful because of rapid temporal and spatial changes.

The selection of the high elevation angle (75°) of the antenna beam for measuring horizontal wind components is influenced by a number of factors:

- For a mechanically-fixed antenna, the elevation angle should be as large as possible to keep the effective aperture large; the aperture projected onto the pointing direction varies as $A_p \cos\theta$ where $A_p$ is the physical aperture and $\theta$ is the steering angle from the physical axis. For a 75° elevation angle and a zenith axis, the projected aperture is only 0.15 dB (4%) less than $A_p$.
- To maximize radar sensitivity by minimizing the range to a given height, the elevation angle should be as large as possible; the range is $h/\sin\theta_e$ so the excess $r^{-2}$ loss is 0.3 dB for a 75° elevation angle.
- The height resolution of the radar depends on the range resolution and the antenna beamwidth; the antenna elevation angle should be high enough so that range resolution determines height resolution, because range resolution can be controlled by system bandwidth whereas beamwidth is fixed by the antenna dimensions. Thus, radar range resolution ($\Delta R$) determines the height resolution if $\Delta R \sin\theta_e > h_m B_2 \times \cot\theta_e$ where $B_2$ is the two-way beamwidth and $h_m$ is the maximum height of interest. For a two-way beamwidth of 3°, a maximum height of 20 km and an elevation angle of 75° a height resolution of 300 m can be achieved.
- The elevation angle should be as high as possible to minimize effects of horizontal gradients in the wind as discussed earlier.

Opposing these factors that mandate elevation angles near zenith are two that favor lower elevation angles:

- For accuracy of wind measurement, the elevation angle should be as low as possible because uncertainty in the measurement of radial velocity causes an uncertainty in the horizontal wind measurement, given by

$$\text{STD DEV}\,\hat{V}_h = \frac{\text{STD DEV}(\hat{V}_i)}{\cos\theta_e}.$$

At 75° elevation angle the uncertainty in the horizontal wind components is 3.86 times the uncertainty of the radial measurement. The mean radial velocity can be measured with an uncertainty of $1/5$ m s$^{-1}$ in typical situations; therefore horizontal wind components can be measured to 1 m s$^{-1}$. The accuracy of horizontal wind measurements degrades rapidly for elevation angles greater than 75°. In addition, bias errors in wind measurements caused by errors in the antenna beam pointing become greater at higher elevation angles.

- At long wavelengths (6–10 m) enhanced radar reflections are observed on a zenith-pointing antenna beam. These reflections are caused by horizontally stratified atmospheric layers; they can be used to detect the height of temperature inversions, at the tropopause for example (Gage and Green, 1979). The intensity of this quasi-specular reflection decreases as the antenna elevation angle decreases from zenith, but if the antenna beam is pointed too close to zenith, the effective beam pointing angle will be biased toward zenith, and this pointing error will bias horizontal wind measurements toward low values. At 15° off-zenith this effect may be negligible (Röttger, 1980) most of the time.

### *b. The 6 m wavelength radar*

This radar is located at Platteville, Colorado, about 50 km north of Denver's Stapleton International Airport; it was developed by the Aeronomy Laboratory of ERL, NOAA, to test new VHF radar techniques (Ecklund *et al.*, 1979). Fig. 9 shows the antenna layout. The large antenna aperture (100 m × 100 m) needed for sensitivity to measure upper altitude winds and to generate a narrow antenna beamwidth (3.5°) is obtained by low-cost construction techniques. There are separate antennas for the three pointing directions. Each antenna consists of 32 rows of dipoles spaced at λ/2. The dipoles are constructed from coaxial cables supported on fence posts about λ/4 above a ground plane. The dipoles are made by interchanging the inner and outer conductor of the coaxial cable every λ/2 (Balsley and Ecklund, 1972). The colinear–coaxial dipole array is fed at the center of each row of dipoles. The rows are all fed in-phase for the zenith pointing beam; the phase is shifted from row to row by changing the length of the feed lines to generate the beams 15° off zenith.

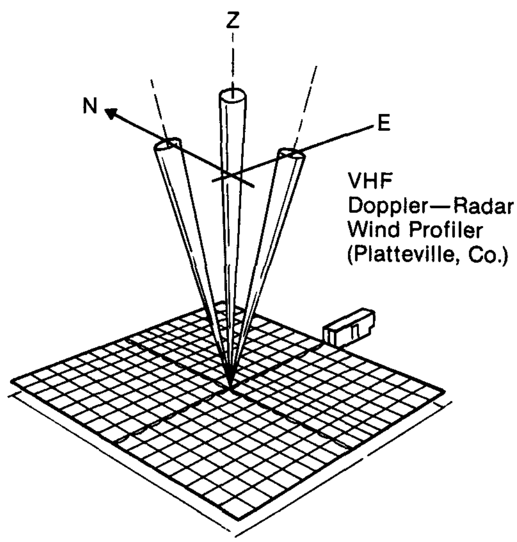


FIG. 9. Crossed array of the VHF radar at Platteville, Colorado; two beams pointing 15° off zenith (to the north and east) are generated by the array; the beam pointing to the zenith is produced by a separate array (not shown).

TABLE 4. Specifications of the 6 m radar.

| | |
|---|---|
| Frequency | 49.92 MHz (6.005 m) |
| Pulse width | 16 μs |
| Pulse repetition period | 2400 μs |
| Peak power | 10 kW (each antenna) |
| Number of heights observed | 13 |
| Range spacing | 10 μs (1500 m) |
| Minimum range | ~2 km AGL |
| Antenna beam-pointing | zenith and 15° off zenith to north and east (simultaneous operation) |
| Unambiguous velocity | 2.44 m $s^{-1}$ vertical mode<br>75.5 m $s^{-1}$ horizontal mode |
| Height sampling interval | 1500 m vertical data<br>1450 m horizontal data |

The operating parameters for the 6 m radar are given in Table 4. The coarse spacing of the sampling gates (10 μs or 1500 m) and the low duty cycle (0.67%) are caused by limitations in the data processor. This radar has operated unattended for about 18 months. Operation cycles between two modes; one is designed for horizontal wind measurement and the other for vertical data. Each mode is used every 5 minutes. These data are auto-dialed by the host computer in Denver (see Section 8) after each mode is completed. Calculation of wind profiles and averaging of profiles are accomplished in the host computer.

### *c. Horizontal wind measurements with the 6 m radar*

Horizontal winds measured by the 6 m radar have been compared with winds measured by rawinsondes, aircraft and another Doppler radar to check the relative accuracy of the measurements. These are major questions regarding the 6 m radar: 1) What are the actual pointing directions of the antenna beams? The pointing directions are very difficult to measure because the antenna is not steerable. 2) Do partial specular reflections bias the effective pointing angles toward the zenith? If there is a problem caused by specular reflections it would be dependent on the particular meteorology being observed and on the height being observed, so it will be difficult to assess. 3) How does the coarse resolution of the radar affect wind measurements?

An example of a profile of horizontal winds, measured by VHF radar at the same time as a sonde launch at the Denver WSFO, is shown in Fig. 10. For comparison the rawinsonde measurements are shown as circles with a unit vector indicating direction. Note

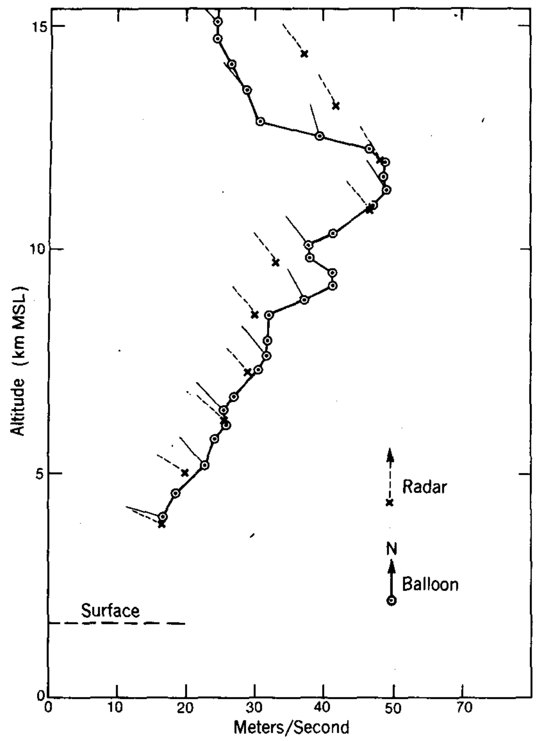


FIG. 10. A wind profile measured by the VHF radar at Platteville, Colorado, compared with simultaneous data from a NWS radiosonde at Denver.

that the two sets of data are not in good agreement for altitudes 40 000–50 000 ft; this may be partly because the balloon drifted about 100 kilometers to the southeast at those altitudes, or by tracking error. Attempts to compare the radar with instrumented aircraft have been unsatisfactory so far because the aircraft contaminates the radar data and because the winds were light and variable when the tests were made.

The best comparisons to date have been made by colocating a microwave (3 cm) Doppler radar next to the 6-m radar and pointing at the same elevation angle. The microwave radar provides a detailed horizontal wind profile but it can operate only when precipitation targets are present. Microwave radar data were analyzed with the Velocity Azimuth Display (VAD) method (Browning and Wexler, 1968). Figs. 11a and 11b illustrate the wind profile comparisons for the orthogonal wind components measured with the two radars. These data were obtained during a spring snowstorm; the 3 cm radar measured the wind using snow particles as a wind tracer, while the 6 m radar measured the wind using backscatter from turbulent eddies of the atmosphere. As the plots show, the microwave radar has much better height resolution and lower minimum height coverage. Some of the wind profiles measured by the 3 cm radar showed very large gradients in height and time; in these cases the 6 m radar measured wind profiles similar to those shown because of the filtering effect of its coarse height resolution. These comparisons indicate that the 6 m radar is operating approximately as expected, but additional data are needed to answer adequately the questions posed above.

An example of continuous wind profiles measured over a 24 h period by the 6 m radar is shown in Fig. 12. These data were acquired during a frontal passage;

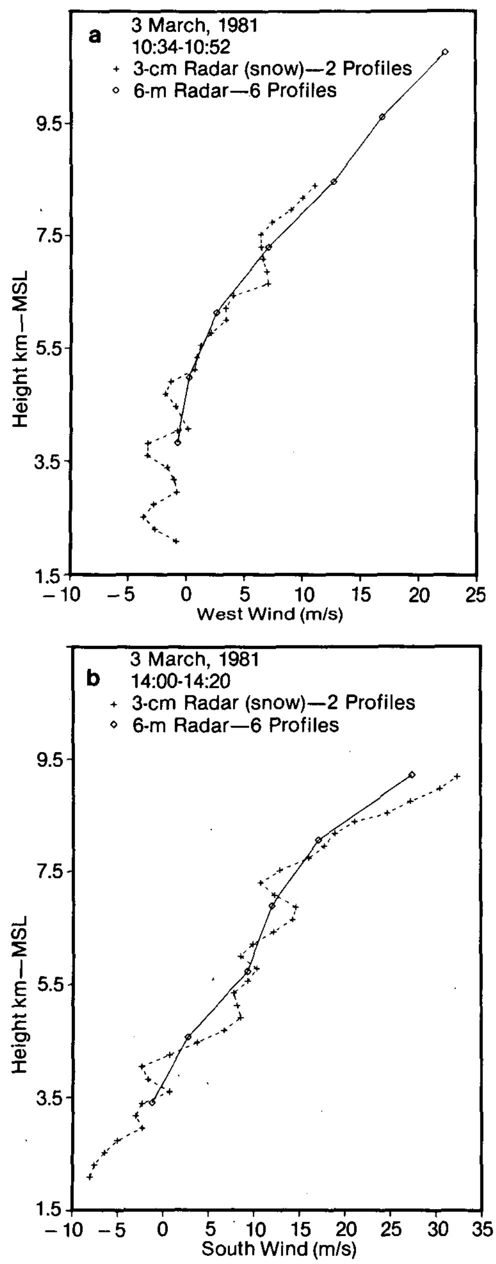


FIG. 11. Comparison of the profiles of the west (a) and south (b) components of the wind measured by the VHF radar at Platteville (solid lines) with data measured by a co-located high-resolution microwave Doppler radar (dashed lines). (Note horizontal scales differ.)

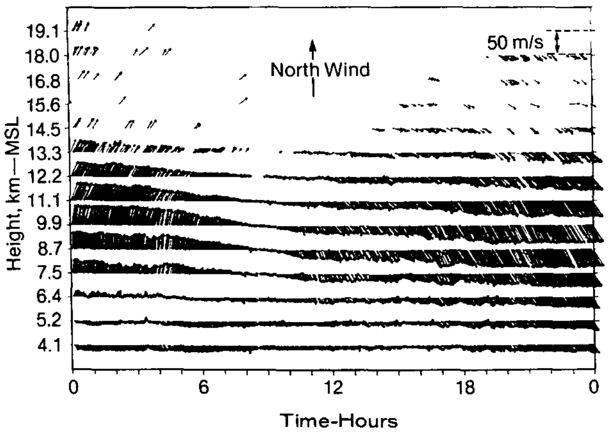


FIG. 12. A 24 h plot for 21 February 1981, showing a reversal of winds in the 8–12 km height range (plot routine through the courtesy of the Aeronomy Laboratory of ERL); measured by the VHF radar at Platteville, Colorado.

the shift from northerly to southerly flow at altitudes above 6 km is evident during the period from 6 to 12 h. In the upper levels there is insufficient signal strength to obtain a measurement. During this time the radar was operated with about 100 watts of average transmitted power and a height resolution of 1150 meters. In a case such as the one shown, it should be possible to measure wind profiles to 20 km altitude if the average transmitted power is increased to 1 kW. Radar-measured winds are frequently contaminated by strong signals obtained from aircraft; data shown in Fig. 12 have been processed using an algorithm to eliminate automatically and in real time, data contaminated by aircraft echoes. The algorithm currently used to average the data and eliminate aircraft interference operates as follows: Twelve estimates of the wind components, obtained during the previous hour, are examined. At each height, the largest set of measurements within 4 m $s^{-1}$ of each other are used to calculate the average wind. If there are not at least four measurements in the set, the data are discarded. The process is updated every 20 min. Both wind components must yield a measurement set that passes the above criterion. The algorithm is a simple version of Random Sample Consensus (Fischler and Bolles, 1981). In addition to eliminating aircraft interference, this algorithm eliminates data if the signal-to-noise ratio is too low to permit a wind measurement. In these cases the radar-measured wind component is a random number, uniformly distributed between plus and minus 75.5 m $s^{-1}$; the probability that both wind components will yield an estimate with noise-like inputs is very small.

An example of the winds measured by the 6-m radar during high-wind conditions in the lee of the mountains is shown in Fig. 13. Rapid changes in speed and direction are evident in the data. A smoothed trend (interpolation) from 1200 to 2300 GMT for the wind speeds at 9680 m MSL would be in error by about 20 m $s^{-1}$ at 1730 GMT.

### *d. Vertical winds measured by the 6 m radar*

Vertical wind measurements are illustrated in Fig. 14. Note that at the start of the record the vertical velocities are very small (0.1 m $s^{-1}$) at all heights. Vertical winds are measured to greater heights (20 km MSL in this case) than horizontal winds because the vertical antenna beam is sensitive to quasi-specular reflections from stable layers. The quiet periods in the record therefore indicate the precision of vertical motion measurements. The very active periods appear to be driven by the synoptic weather; the gravity waves apparent in Fig. 14 are probably caused by

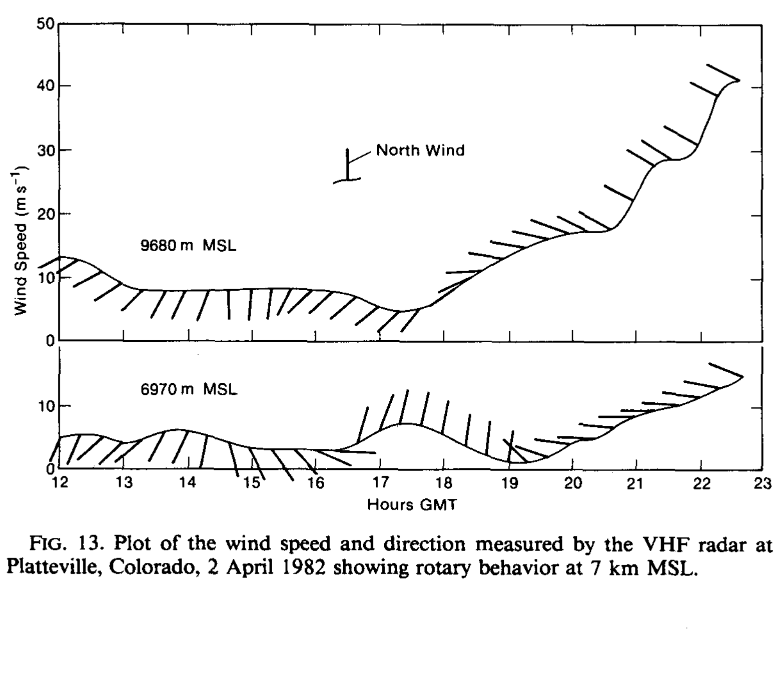


FIG. 13. Plot of the wind speed and direction measured by the VHF radar at Platteville, Colorado, 2 April 1982 showing rotary behavior at 7 km MSL.

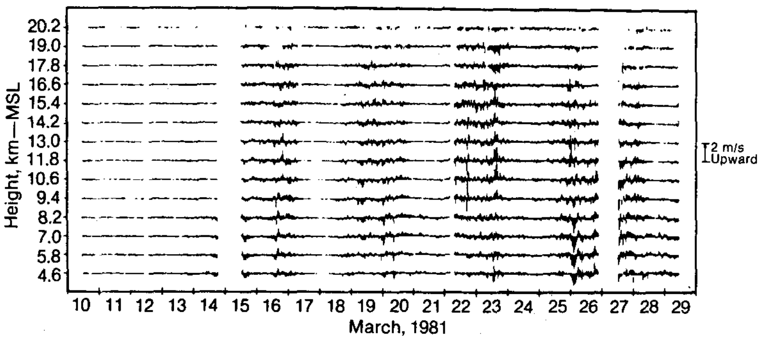


FIG. 14. Example of vertical winds measured using the zenith beam of the VHF radar at Platteville, Colorado. Note the strong downward flow (~1.5 m $s^{-1}$) at the 4.6–8.2 km levels during the first hours of 26 March 1981.

zonal winds over the continental divide (Ecklund *et al.*, 1982). At present the primary purpose of the data obtained with the zenith-pointing antenna is to measure the height of the tropopause (see below), but direct measurement of vertical motions with temporal averaging to remove wave effects may prove valuable in forecasting mesoscale convection.

### *e. Tropopause height measured by the 6 m radar*

The 6 m wavelength radar also measures the height of the tropopause; averaging times are similar to those used for wind observations. The partial specular reflections that are observed with the zenith-pointing antenna beam are from stable atmospheric layers; the tropopause is the most important of these layers, and the reflection from this layer can be identified and its height measured (Gage and Green, 1979). The tropopause height is an important parameter for the local forecaster concerned with the development of deep convection. It is equally important in the Profiler itself in the retrieval of temperature profiles because if the tropopause height is known, then significant improvement in the accuracy of radiometrically-measured temperature profiles is obtained (see Section 7). Fig. 15 shows a comparison of the height of the tropopause as measured by the 6 m radar and by radiosonde. Two algorithms have been used to determine tropopause height from the radar data (Westwater *et al.*, 1983); one uses a model for the expected reflectivity that includes the lapse rate; the measured profile of reflected power is compared with a model of the expected reflected power for a 2 K $km^{-1}$ lapse rate. The other method uses the temporal and spatial correlations of the echo power to measure the height of persistent reflecting layers and uses statistical knowledge of the expected height of the tropopause to identify the proper layer as the tropopause. The latter algorithm was used for the data in Fig. 15. The discrepancies in the measurements at the

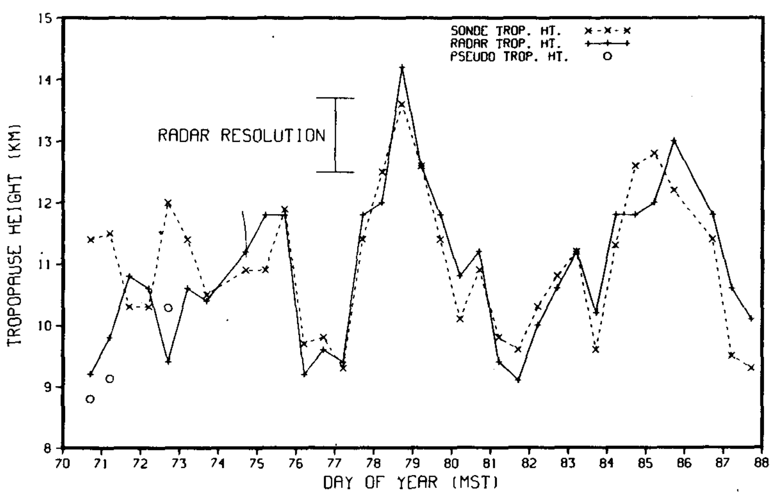


FIG. 15. Tropopause height, measured in real time by the VHF radar at Platteville, Colorado (solid line) and by the Denver radiosonde (dashed line). Heights shown by the three open circles are for inversions that do not quite satisfy the WMO standard definition of the tropopause.

start of the period (days 70 to 73) are in part caused by the poorly-defined tropopause that existed during that time. Examination of the radiosonde data showed that temperature gradients existed in the profile that nearly met the WMO definition of the tropopause—these are labeled as pseudo-tropopause heights in the figure.

### *f. The 33 cm radar*

Construction of this UHF radar, located at Stapleton Airport, Denver, is just being completed; it measures winds with better height resolution and at lower minimum heights than the 6 m radar, but the maximum height at which winds can be measured will be less. The characteristics of this radar are listed in Table 5. The antenna is an offset paraboloidal reflector that uses offset feeds for beam steering. Three beams, in the same geometrical configuration as the 6-m antenna, are produced (i.e., to zenith and 15° off zenith). Fig. 16 shows the antenna system (Earnshaw *et al.,* 1983). The three pointing directions are observed sequentially rather than simultaneously as with the 6 m radar. In addition, at each pointing direction the radar will operate in high (1 $\mu$s pulse width) and low (4 $\mu$s pulse width) resolution modes. Low-level winds will be measured every 90 m and upper level winds every 300 m in altitude.

The 33 cm radar has a solid state transmitter; the peak power is relatively low and the average power (duty cycle) is relatively high. Because of the high pulse repetition frequency, integration of video samples can be used to increase the SNR; in the low resolution mode for example, the signals received from 200 consecutive pulses are added to increase the SNR by 23 dB. Video integration is also used with VHF radars but normally cannot be used with UHF radars because the pulse repetition frequency is too low with vacuum tube pulse transmitters. Doppler velocities are measured with spectral processing (Fast Fourier Transform) in a minicomputer. The radar is controlled by computer with an interface unit that selects the antenna pointing, pulses the radar, and samples and integrates the received signal. The interface will also be used with VHF radars being built for the Colorado Mesoscale Network (see Section 9d).

Preliminary tests with this radar indicate that wind profiles should be measured routinely to 8–10 km MSL with a 4 $\mu$s pulse width. The radar is complete except for the data system. A sample wind profile measured with the 33 cm radar is shown in Fig. 17.

TABLE 5. Specifications of the 33 cm radar.

| | |
|---|---|
| Frequency | 915 MHz (0.327 cm) |
| Pulse width | 1, 4 $\mu$s |
| Pulse repetition period | 30, 64 $\mu$s |
| Peak power | 5.5 kW |
| Number of heights observed | 24 |
| Range spacing | 0.67, 2 $\mu$s (90, 300 m) |
| Minimum range | (0.3, 1 km) |
| Antenna pointing | zenith and 15° off zenith to north and east (sequential) |
| Unambiguous velocity | ±52, ±77 m $s^{-1}$ (horizontal)<br>±15, ±15 m $s^{-1}$ (vertical) |
| Height sampling interval | 90, 300 m |

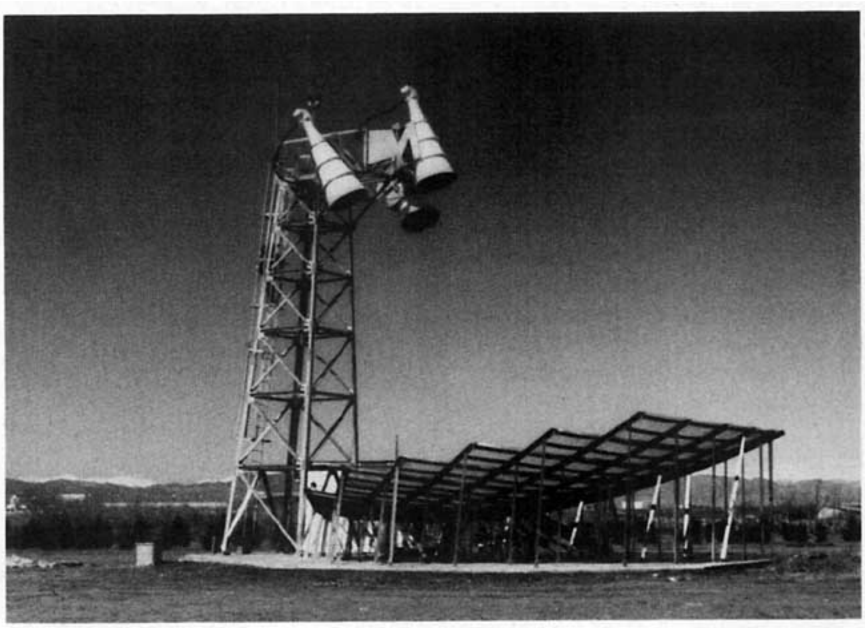

FIG. 16. The triple-beam antenna of the UHF radar at Stapleton Airport, Denver, Colorado. The three conical feed horns and the offset paraboloid generate two beams 15° off zenith, to the east and north, for profiling horizontal winds and a zenith beam for vertical velocity and intensity measurements.

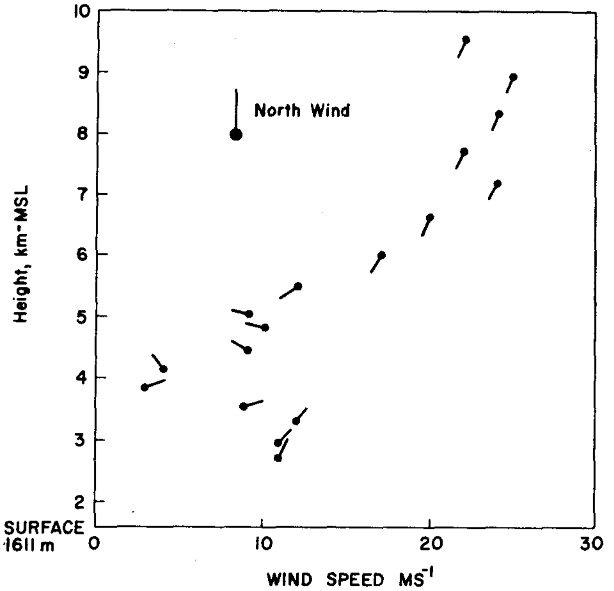


FIG. 17. An initial measurement of a profile of horizontal winds by the UHF radar at Stapleton Airport. Note the development of shear in the range 3.5–4.5 km MSL.

The radar is located adjacent to the NWS radiosonde facility at Denver, so it will be much more meaningful to compare wind measurements from this radar and from radiosondes, as opposed to the 6 m radar which is located some 50 km away.

## 7. Combined profiling

### *a. Joint active/passive profiling*

Passive microwave radiometric observations of atmospheric brightness temperatures are characterized by excellent sensitivity (~0.1 K) and absolute accuracy (~0.5 K), and possess the added feature of excellent temporal resolution. However, when the passive observations are transformed to temperature profiles, the lack of vertical resolution may present a problem for some applications. As we have seen in Section 5, resolution of the passive system is adequate to recover significant features of ground-based or nocturnal temperature inversions but is not adequate to recover the sharp details of elevated inversions.

Microwave radar (Gossard *et al.*, 1971) is known to be sensitive to sharp gradients of refractive index in the lower atmosphere. These gradients are, in turn, usually indicative of the heights of significant levels, such as the base of elevated temperature/humidity inversions, or the height of nocturnal inversions. In the upper tropospheric and lower stratospheric regions, strong VHF echoes of a specular nature have been observed regularly. The region of strong reflectivity gradients has been directly associated with the tropopause (Gage and Green, 1979; see also Section 6a).

It is now becoming clear that knowledge of heights of significant and persistent changes in temperature (or humidity) can be used to improve retrieval of radiometric profiles. It has been shown (Westwater, 1978; Westwater and Grody, 1980) that a simple extension of linear statistical inversion (Westwater and Strand, 1968) can naturally assimilate significant height information into the retrieval process. Essentially, this extension restricts *a priori* profiles that are used to construct retrieval coefficients to a subset containing profiles that possess only the desired significant height within a given altitude band. Linear retrieval coefficients then are derived from the restricted subset in the usual way. Consider, for example, a radar-indicated height of the base of an elevated inversion at 2 km, and a resolving power of the radar of ±200 m. Then, to couple the radar information with that of the radiometer we would use radiometric retrieval coefficients derived from an *a priori* ensemble of profiles that contained base heights of elevated inversions from 1.8 to 2.2 km. In practice, the resolution window's width must be consistent with the resolution of the radar (see Section 6), and the window should be large enough to include a sufficient number of *a priori* profiles to allow construction of the retrieval coefficients with statistical confidence.

This technique has been applied to numerous computer-simulated retrievals; a typical one is shown in Fig. 18. Here both radiometer and radiosonde data are measured (Decker *et al.*, 1978), but the inferred radar height was simulated by assuming that the height of the base of the elevated (tradewind) inversion was known to within 20 mb (~200 m). Note

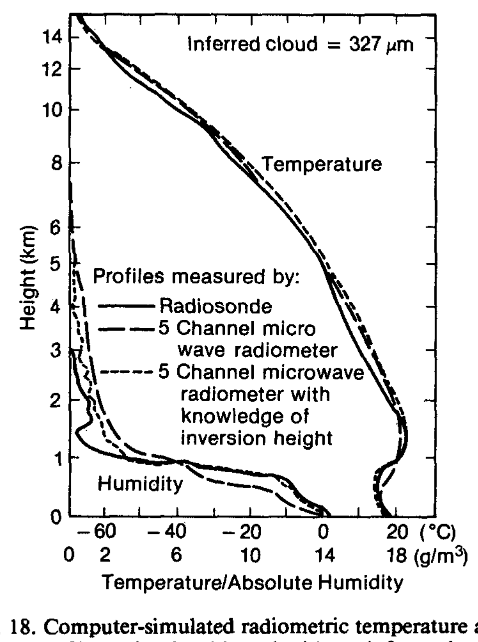


FIG. 18. Computer-simulated radiometric temperature and water vapor profile retrievals with and without information on the height of the inversion at about 1 km.

the dramatic improvement in accuracy in the retrieval temperature and humidity profiles when the height information is included.

In addition to this computer simulation, field experiments (Decker, 1978) have been conducted using both active and passive sounders. These experiments provide an example of the use of clear air returns obtained by a 10 cm wavelength radar (Chadwick *et al.*, 1976) in improving temperature profile retrieval (see Fig. 19). These data were obtained at the Boulder Atmospheric Observatory (BAO) near Boulder, Colorado, 6 September 1978. The radiosonde profile is from a conventional system operated by the National Center for Atmospheric Research (NCAR). The radiometric data were measured with a ground-based version of the SCAMS radiometer which was operated by personnel from the Jet Propulsion Laboratory. These measurements include zenith radiation at five frequencies plus 55.45 GHz measurements at a zenith angle of 59.3 degrees. (This sixth observation was taken to simulate use of the 58.8 GHz zenith channel used in the Profiler system.) By using these six measurements and measurements of surface temperature, pressure and relative humidity, the profile designated "Radiometer, No Height Information" of Fig. 19 was obtained. As expected, this profile smooths the elevated temperature inversion evident in the radiosonde profile. At the time of the radiometric measurement, a persistent echo was observed at 190 m above the surface by a 10 cm wavelength radar. We now include this information in the temperature profile retrieval process by assuming that the radar echo represents the base of an elevated temperature inversion. Statistical coefficients were derived from the set of *a priori* profiles that contain elevated temperature inversion bases between 10 and 30 mb pressure difference from the surface. The resulting profile, designated "Radiometer with Height Information" of Fig. 19, now exhibits the structure of the radiosonde profile.

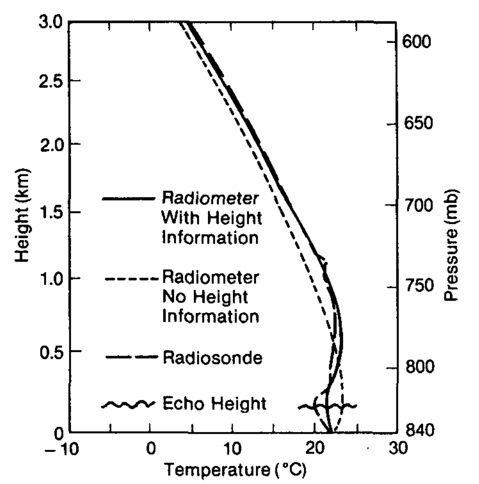


FIG. 19. Temperature profile retrieved with and without radar-measured height of an inversion 6 September 1978, Erie, Colorado, compared with local radiosonde.

In addition to measuring low altitude features of temperature, radars are also capable of measuring tropopause height (Gage and Green, 1979) as discussed in Section 6a. The tropopause height information can be inserted into a temperature retrieval algorithm using the restricted-ensemble technique discussed above. The data shown in Fig. 20 were used in the retrieval algorithm in the following manner: a set of retrieval coefficients was associated with each measured tropopause level; these coefficients were constructed from an ensemble of temperature profiles whose tropopause pressures were restricted to a ±20 mb interval, centered about the measured point. In Fig. 20, two radar/radiometric (active/passive) retrievals, obtained with this technique, are compared with the radiometric retrieval only and with coincident radiosonde profiles. Note that the active/passive profiles improve substantially in the vicinity of the tropopause, and that in both cases the improvement persists over an extended altitude range. The rms error statistics, for the 21 cases for which simultaneous radar, radiometric and radiosonde data have been compared, are shown in Fig. 21. As much as 2 K rms improvement in retrieval accuracy is achieved by the addition of tropopause height information. The heights of pressure surfaces, using profiles incorporating inversion-height correction, have not yet been made.

Although the improvement in retrieval of temperature profiles with the joint active/passive technique is evident, work remains before it is applied in a real-time operational mode. Echoes measured by the active sounder may arise from atmospheric properties different from those assumed here, hence further experience must be gained before this technique is applied with complete confidence.

Another potentially useful combined active/passive technique involves addition of cloud-base height (CBH) measurements, such as those obtained from a ceilometer or radar, to the radiometric observations. The CBH observation could improve retrieval accuracy in at least two ways: 1) the relative humidity exceeds 85% at cloud base and thus the measurement could provide a nearly exact constraint on the humidity profile retrieval and 2) knowledge of CBH, along with the temperature profile as measured by the Profiler, could decrease the uncertainty in the estimation of cloud temperature. This uncertainty is one of the limiting factors in moisture retrieval (Westwater, 1978).

In addition, if cloud-base temperature could also be measured, that value (along with knowledge of CBH) could provide a useful constraint on the temperature profile. An infrared (IR) radiometer, operating in a suitably transparent clear-air absorption

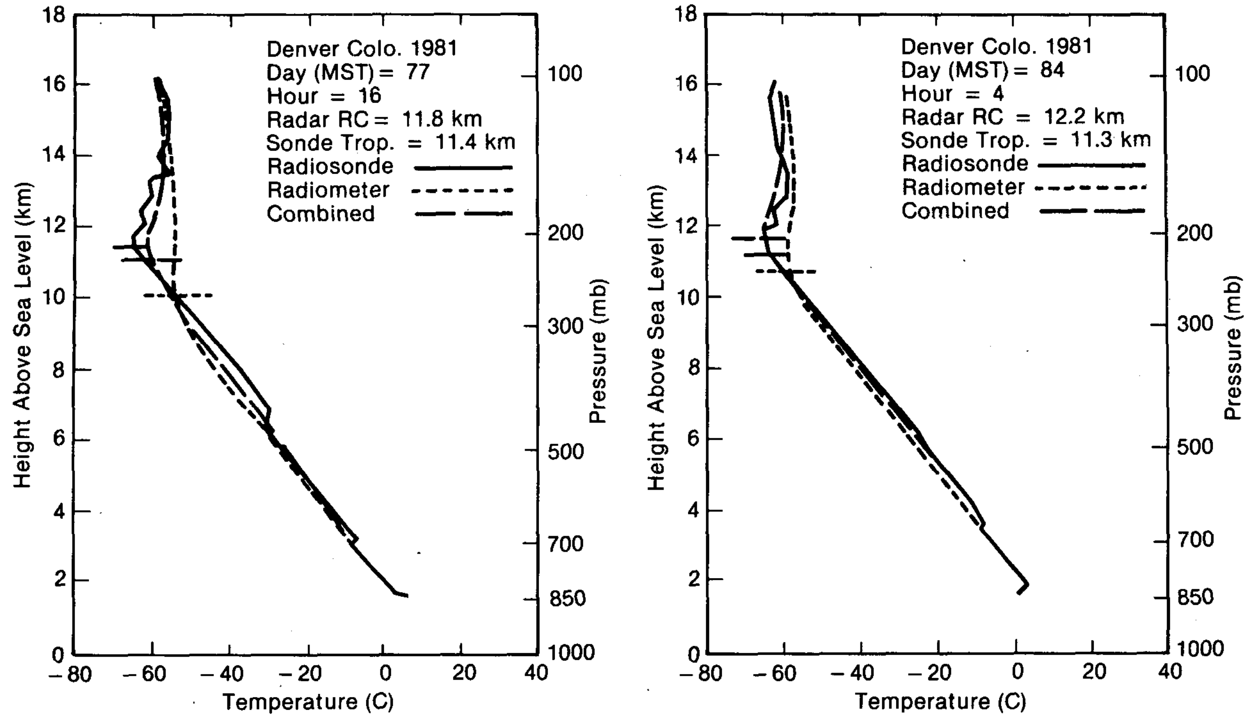


FIG. 20. Temperature profiles retrieved using radiometric data only (dotted lines) and joint retrieval including VHF radar-measured height of the tropopause (dashed lines) compared with radiosonde (solid lines).

band, may provide the necessary temperature accuracy during nonprecipitating conditions. Complementary observations of cloud liquid, as provided by the 20.6/31.65 GHz radiometer, could be used to reject IR observations of non-opaque clouds. In addition, the clear-air transmission and emission from cloud base to ground could also be corrected to first order by knowledge of the temperature and humidity profiles obtained from the Profiler. This relatively simple technique is currently under investigation.

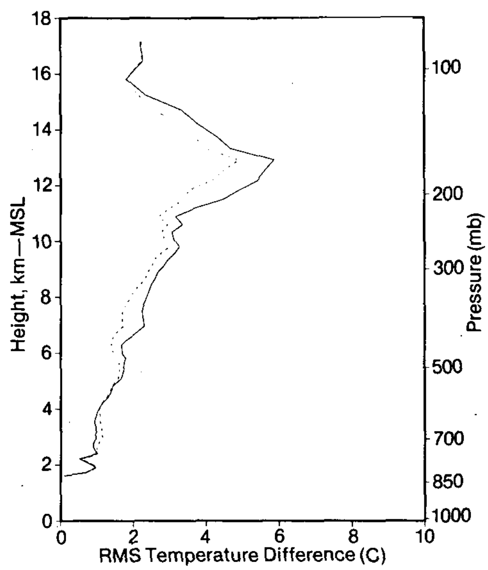


FIG. 21. Root-mean-square differences between profiles retrieved from radiometric data only (dotted line) and radiosonde (solid line), and a similar comparison using radiometric data plus radar-determined tropopause height (dashed line); for 21 samples during March 1981 at Denver, Colorado.

*b. Combined satellite/Profiler retrievals*

We have recently started studying the feasibility of combining satellite and Profiler data to yield improved temperature profiles. Initial work by Westwater and Grody (1980) showed that retrieval accuracies generally better than 2.0 K rms could be obtained from the surface to about 300 mb by using combined satellite/ground-based microwave sensors. If, in addition, radar measurements of tropopause height are available (see Sections 6a and 7a), the range of accurate sounding could be extended to 100 mb.

As an initial step in combining profiles from ground and satellite based sensors, we have compared accuracies of Profiler retrievals and NOAA-6 and NOAA-7 satellite data, and a few VAS soundings. The NOAA-6/7 soundings are derived from microwave and infrared instruments aboard orbiting satellites (Smith *et al.,* 1981). A typical result is shown in Fig. 22. Note the good agreement of the Profiler retrieval with the radiosonde in the region below ~200 mb and the good agreement of the satellite with the radiosonde above this level. A statistical comparison of rms differences between each of the

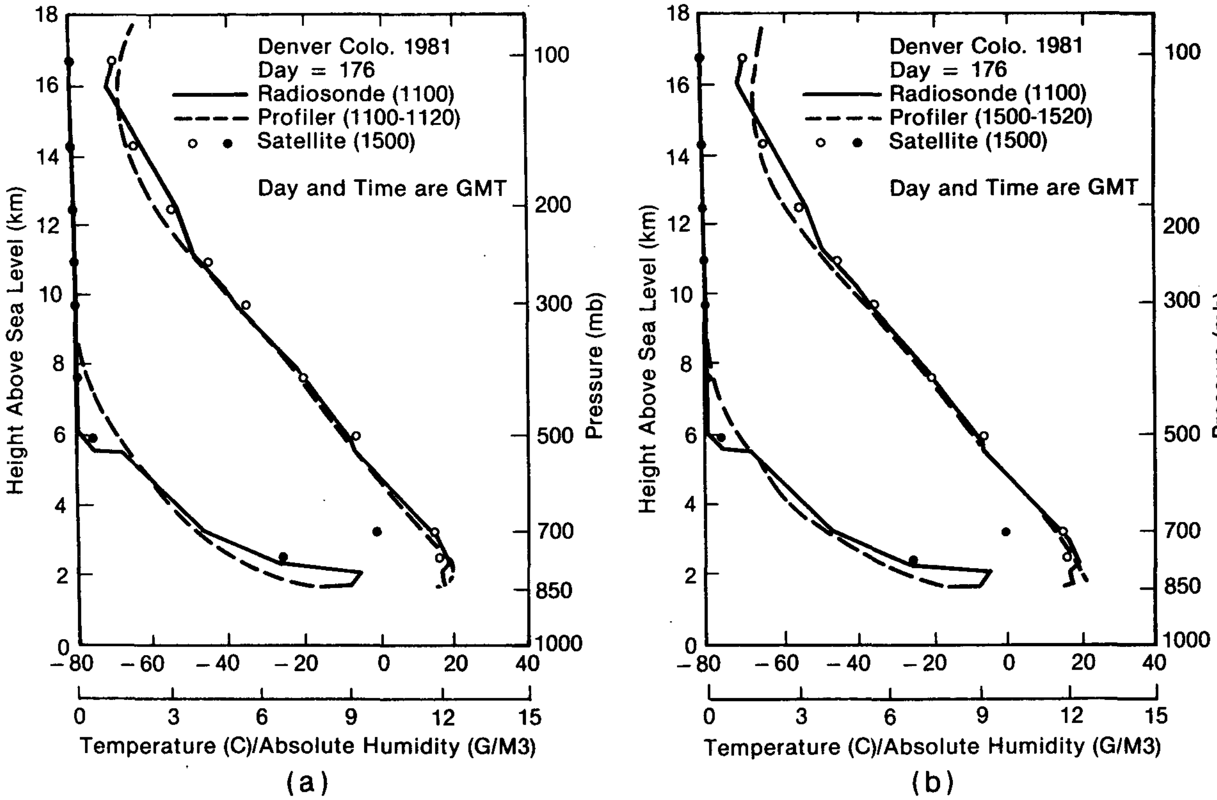


FIG. 22. Comparison of a sounding taken from the NOAA-6 satellite with data from the Profiler and the Denver radiosonde: (a) Profiler and radiosonde times coincident, (b) Profiler and satellite sounding times coincident.

two sounders and the radiosonde is also being conducted. In Fig. 23, the rms statistics for 131 profiles obtained during 1981–82 are shown. It is suggestive from the curves that the two sounding systems can effectively complement each other in constructing a more accurate, combined profile.

Another source of satellite soundings is the VAS, operating from geostationary orbit on the GOES-5, and operated by NESS at the University of Wisconsin. This sounder operates in the infrared, therefore, in contrast to NOAA-6/7, does not contain microwave channels, and hence cannot routinely sound in the presence of all clouds. On 1 July 1981, VAS, then in a trial period prior to the operational phase, made special dwell soundings for the Denver area; the weather conditions were clear. Three profiles were obtained; a typical one is shown in Fig. 24. The retrieved temperature profiles are in reasonable agreement with the radiosonde, but the satellite humidity profile, when integrated with height, yields a precipitable vapor that is 50% higher than that obtained with the Profiler or the Denver radiosonde launched a few hours earlier.

To combine satellite and Profiler sounding data most effectively, it is essential to establish the covariances representing retrieval errors of each system. Since such covariances do not seem to be published for the satellite case, we are currently constructing them for satellite soundings over Denver, Colorado.

We also plan to use the Colorado Mesoscale Profiler Network (see Section 9d) to test the validity of the combined Profiler/VAS interpolation technique, after completion of all Profilers near Sterling, Craig and Cortez, and the addition of a fourth outlying site in southeastern Colorado (probably at Lamar). Interpolations for Denver, using data from VAS and the four outlying sites, will be compared with the data measured by the Denver Profiler.

## 8. The data system

### *a. Structure*

The Profiler data system uses several small to medium scale mini- and microcomputers in various subsystems. The central-node, or host computer is a Data General (DG) Eclipse S-250/IAP located at the Profiler building, NWS WSFO, Denver (see Figs. 1 and 2). An LSI-11 node samples the signals from the radiometers, processes these data into brightness temperatures, and passes 2 min averages to the host. A micro-logger node samples and averages data from the surface meteorological instruments and passes 10-min averages to the host and to the radiometer LSI node in parallel. A remote node controls the Platte-

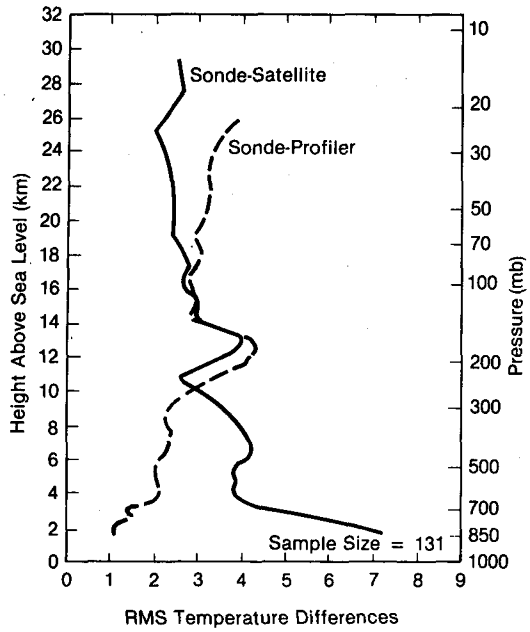


FIG. 23. Root-mean-square statistics of differences between simultaneous data measured by the NOAA-6/7 sounders and Denver radiosonde (circles), and between the Profiler and Denver radiosonde (triangles).

ville radar and processes radar data into wind-component vectors for transmission to the host, at request of the host computer.

In the host system a "hub" process performs multiple asynchronous tasks that acquire the data blocks from each external node, and makes these data globally available to all other processes within the system. One such task auto-dials the remote radar node at Platteville (see Section 6a) every 2.5 min and requests wind components. The other remote nodes, the mesoscale network stations (see Section 10a), will be dialed once each hour. The wind components are passed on for processing including application of an aircraft reflection-rejection algorithm (see Section 6a). Processed data are then forwarded again for further processing within the system. This "hub" concept allows many processes within the system to make use of the data simultaneously and asynchronously.

*b. Examples of user formats*

The "PROFILER" and "PROFS" processes are discussed here as examples of simultaneous data formatted for users.

Outputs of the PROFILER process requests the radiometric data set from the hub, the surface micro-

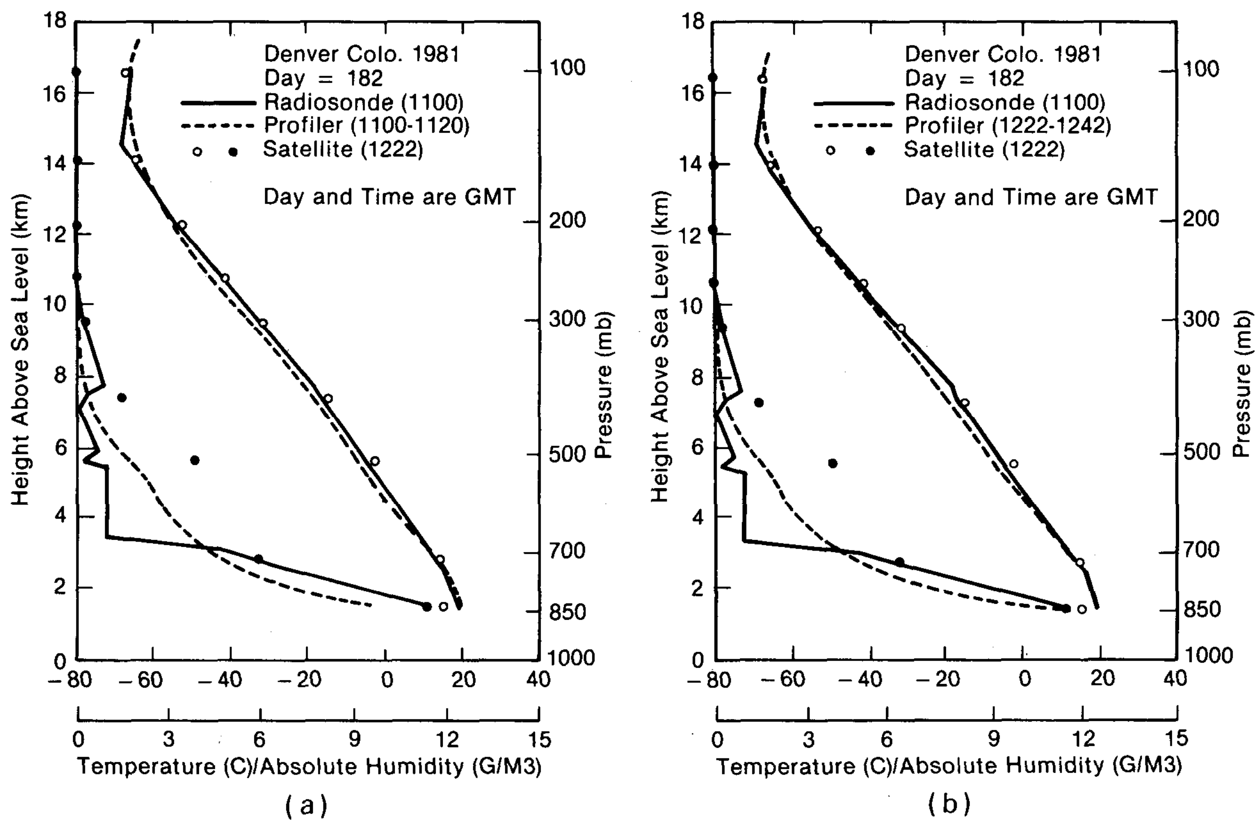


FIG. 24. Comparison of a sounding taken by the VAS on GOES-5 with Profiler and Denver radiosonde profiles: (a) Profiler and radiosonde times coincident, (b) Profiler and satellite sounding times coincident.

logger data set, and the winds from the Platteville node. These data are processed into a hardcopy plot output that consists of temperature, humidity, and wind profiles and time series of integrated liquid, water vapor and 500 mb height. An example of the hardcopy is shown in Fig. 25. This display, called the Profiler Monitor, serves primarily to determine that all instruments of the Profiler are functioning properly. The time interval in the example shown is 20 min and the quantities are 20 min averages, but they can be plotted at any user-requested time interval from 5 to 60 min.

On the left half of Fig. 25 (the Monitor output), is a 16 h time (GMT) series of precipitable water vapor ($V$), in cm, read from the upper abscissa (1 to 5). For the integrated liquid in the zenith ($L$), the same scale applies, but in units of mm; numerous liquid-bearing clouds are present in this example, and ~2.5 mm of rain fell during the period. The height of the 500 mb level is indicated by a 5, and the abscissa running from 5.1 to 6.1 km applies. All of these data are 20 min averages.

The surface pressure (832 mb in this case) is shown in the lower-left corner of the upper-right quadrant of the figure, and pressure (mb) is the ordinate. The profile of temperature (the $T$'s) is related to the abscissa covering the range −80 to 40°C, whereas humidity ($H$) is in g m$^{-3}$ on the scale from 0 to 15. The time series of 500 mb height is obtained by integration of these profiles from the surface.

The wind profile measured by the 6-m wavelength radar (the lower-right quadrant) has an abscissa scale for speed ($S$) of 0 to 6, in tens of m s$^{-1}$; the ordinate is in km MSL. In this example, the maximum speed of just over 30 m s$^{-1}$ occurs at ~11 km altitude. The wind direction ($D$), for which the scale indicating the cardinal points of the compass applies, changes roughly from NNW to W with increasing altitude. Data from the UHF Wind Profiler that exhibits high resolution in altitude (Section 6b) is not yet included

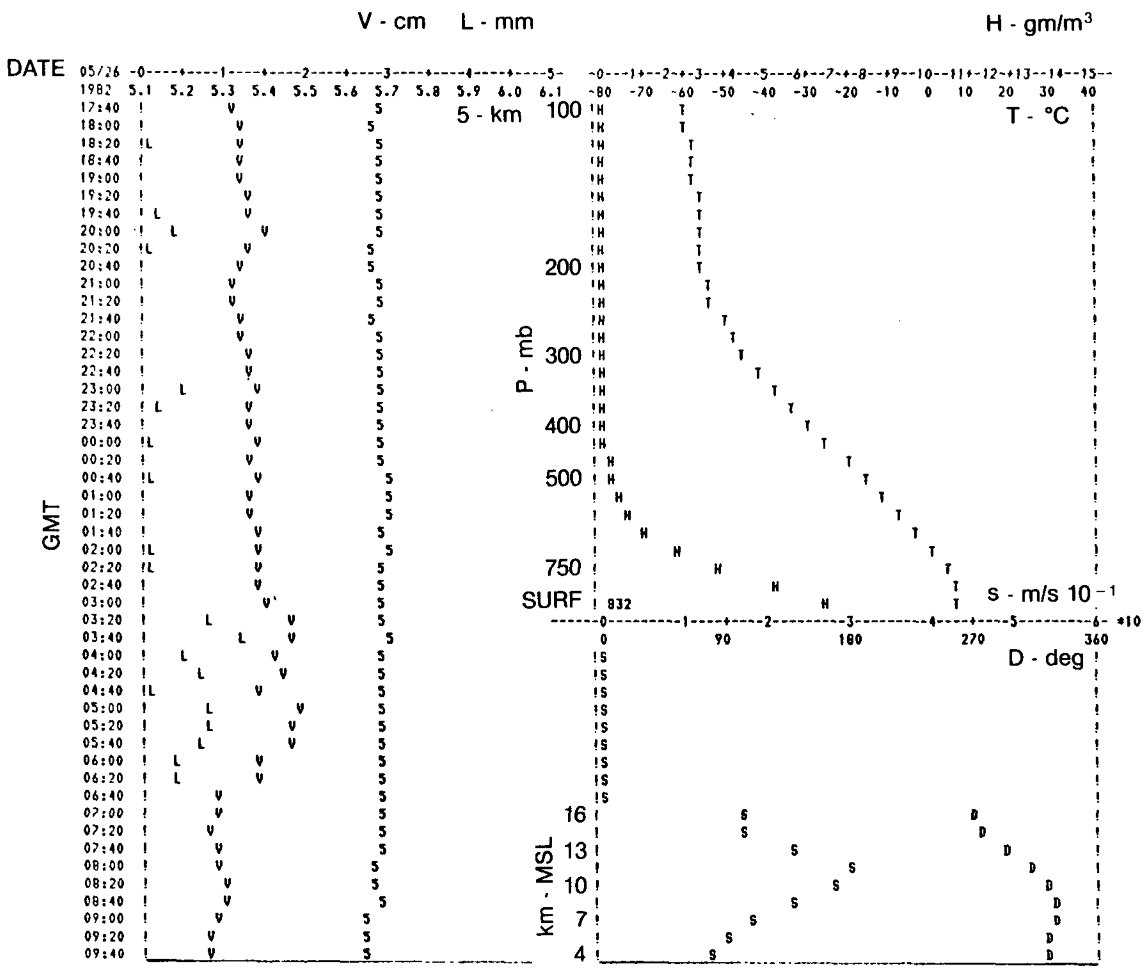


FIG. 25. Hardcopy output of the Profiler Monitor. These sheets are plotted every 20 min; the profiles on the right apply to the last time entry (0940) in the column on the left; see text for description and definition of symbols and units.

on the Monitor display, because software is incomplete. Likewise, time series of tropopause height will not be included until definitive tests of the algorithm for automatic identification of the tropopause are complete.

The "PROFS" process gathers from the hub the same information as that displayed on the Monitor, but converts it into more detailed profiles (e.g., 80 heights as opposed to 30 for temperature and humidity, and 2-min resolution of water vapor and liquid rather than 20-min, for observing the passage of clouds). These data are transmitted in tabular format to the Prototype Regional Observing and Forecasting Service (PROFS) data-base center via phone line. This stream of data can also be sent at any user-requested interval from 5 to 60 min.

The concept of a central hub of acquisition allows for easy expansion of the user community, whose size is limited only by the size of the host computer. This centralized process also lends itself to validity cross-checking of data sets, and to relatively straightforward error detection and recovery.

### *c. Additional processing*

Although the host computer processes the remotely sensed data, and automatically edits it for quality (with the aircraft reflection-rejection algorithm, for instance), several other special computer programs require implementation for real-time provision of improved profiles, etc.:

- The joint active/passive algorithm, utilizing radar-measured inversion heights (Section 7).
- Adaptive coefficients for the radiometric retrieval process (Section 5f).
- Further time series of special variables, such as tropopause height (Section 6a), turbulence, stability indices.

Further processing is also anticipated when data sets from the Mesoscale Network (Section 9d) are incorporated, and when real-time combined profiling with satellites (Section 7b) is initiated.

## 9. Potential applications of the Profiler system

### *a. Applications to research*

The fact that the Profiler system monitors wind, temperature, and humidity profiles *continuously in time* constitutes a unique capability. It therefore extends the available information on the temporal variability of the atmosphere as a function of height by one or two orders of magnitude. An example is the work of Hogg *et al.* (1981), which provided information on the spectrum of precipitable water vapor to $10^2$ cycles per day—i.e., two orders of magnitude beyond that available (without aliasing) from the twice-per-day radiosonde network.

The high temporal resolution of the Profiler therefore makes it particularly suitable for research on those short duration meteorological phenomena not adequately described by current radiosondes networks. Examples include land–sea, lake–shore, and mountain–plains circulations; weather fronts; thunderstorms; chinook wind storms.

### *b. Applications to development*

Tests of the Profiler system suggest that once its accuracy is fully determined, it will have certain advantages when used in a comparison mode to evaluate the performance of other sensors. These include the continuity of the data in time and the fact that the measurements relate to well-determined positions in space and time (unlike measurements from the radiosonde system, which takes more than 30 minutes to reach the tropopause, and is typically carried laterally by the wind from the launch site during its ascent). However, it is important to recognize that the prototype Profiler does *not* have the height resolution of most *in situ* sensors.

### *c. Applications to weather forecasting*

A nationwide array of Profilers could provide upper air data continuously in time at spacings comparable with those of the present radiosonde network, i.e., at spacings of about 350 km. Such a data set would find uses on many time scales, ranging from "nowcasting" (information on the present state of the atmosphere over the United States) to numerically based weather predictions for periods up to a few days.

#### 1) NOWCASTING

A national network of Profilers, coupled by an effective communication system to a central computer, could provide continuous data on the state of the atmosphere over the United States. Such data, after appropriate analysis and processing, could be used as input to the National Meteorological Center (NMC) models and special regional models. In addition, the data could be made available as continuously updated "nowcasts" to other users, both local and national, including NWS forecast offices, private meteorologists, airlines and any others authorized to receive them.

#### 2) VERY SHORT TERM FORECASTING (1–6 HOURS)

An important gap in weather forecasting exists between the time domain for which nowcasting and short term extrapolations (often good only to 1 or 2 hours) and the time domain for guidance products obtained by numerical weather prediction techniques. These guidance products are currently updated only twice per day, and (because of time expended in data acquisition, analysis and model runs) are rarely based on data less than 6 hours old.

The continuously available upper air data from the Profilers could contribute to forecasts on this very short time period in several ways. These include their use to check and update the NMC numerical guidance, and also as critical inputs for relatively simple, locally specific, physical models or statistical algorithms to be operated upon demand at the local forecast office.

3) MESOSCALE NUMERICAL WEATHER PREDICTION MODELS (IN COMBINATION WITH VAS GEOSTATIONARY SATELLITE SOUNDINGS)

Currently, radiosondes are routinely released twice daily by the NWS; that frequency determines the frequency with which the NMC Limited Fine Mesh (LFM) model is initialized. The continuity of the Profiler data would permit the LFM and mesoscale models to be initialized more frequently (e.g., once per 6 hours), and at a time under flexible control by NMC, rather than that fixed by international agreement (i.e., 0000 and 1200 GMT). There is also potential for incorporating time tendencies from the Profiler data into analysis and initialization procedures.

Currently, there exists a major effort to develop mesoscale models that might eventually lead to operational numerical weather prediction on the mesoscale. The problem of how to obtain the data required to initialize such models (operating over domains of 1000–2000 km, with grid spacing of perhaps 30–50 km) is a very real one. It is believed that the combination of a national array of ground-based Profilers, plus the Visible and Infrared Atmospheric Sounder (VAS) geostationary satellite soundings, could make a valuable contribution to such data sets. This combination has great potential, because each system has strengths that complement the weakness of the other. The VAS data are least accurate near the ground where the Profiler data are most accurate. The most accurate Profiler data are its wind profiles; the VAS satellite cloud and moisture images provide relatively limited wind data. In addition, the Profiler temperature/humidity data is obtained by microwave radiometers and therefore is largely unaffected by clouds, while the data obtained by infrared radiometers are strongly affected by clouds. As shown by Westwater and Grody (1980), the profiles resulting from a combination of ground-based and satellite-based radiometers are significantly more accurate than those produced by either system alone.

By using a combination of an array of Profilers, plus VAS, it should be possible to achieve profile data of good accuracy with high time resolution at each Profiler site. The spatial resolution of such profiles would of course be determined by the number of Profiler stations and would probably be about an order of magnitude poorer than that required to initialize mesoscale models using grid points at spacings of 30–50 km. The question of how to interpolate between Profiler stations is therefore critical. We believe that the capability of the VAS satellite to measure horizontal gradients of moisture or temperature, especially when supported by a reasonably dense array of surface weather sensors, should be used to guide this interpolation. In this way, we anticipate that at some time during the 1990's it should be possible for the NWS to issue numerical weather guidance products based on fairly frequent (e.g., four times per day or more) initialization of relatively high resolution mesoscale models.

4) MEDIUM RANGE (>1 DAY) WEATHER FORECASTING

In addition to providing NWS with the possibility of extending model initialization to smaller time and space scales, the Profiler should have considerable beneficial impact on existing medium range (>1 day) numerical weather guidance products. This results from three main aspects of the Profiler data: 1) the improved accuracy of winds and the accurate total precipitable water vapor data (compared with sonde and satellite data), 2) the availability of additional types of data, including integrated liquid water, but especially including the ability of the combined VAS/Profiler system to provide temporal averages and time derivatives, and 3) the ability of the VAS/Profiler system to provide data more frequently and at times under NMC control.

### *d. Mesoscale Profiler Network*

Work has started on installation of a Mesoscale Network of Profilers in Colorado to test the impact of the additional upper air data on the prediction of weather at Denver. The locations of the network stations, chosen by two mesoscale meteorologists and an operational forecaster, are shown in Fig. 26. The stations near Sterling, Cortez, and Craig, are located (approximately) in three corners of the State of Colorado. The two western stations are over the Rocky Mountain range from Denver; Sterling is on the relatively flat eastern plain. As indicated in the figure, the initial installation will comprise Humidity and VHF Wind Profilers. The latter will operate at the same radio frequency as the Platteville radar (Section 6a), but will have somewhat wider bandwidth (for improved height resolution in the wind profiles), and antennas of one-fourth the area. A station at Lamar may be instrumented in the future.

The dashed lines in Fig. 26 indicate telephone line communications for access of the data. The stations

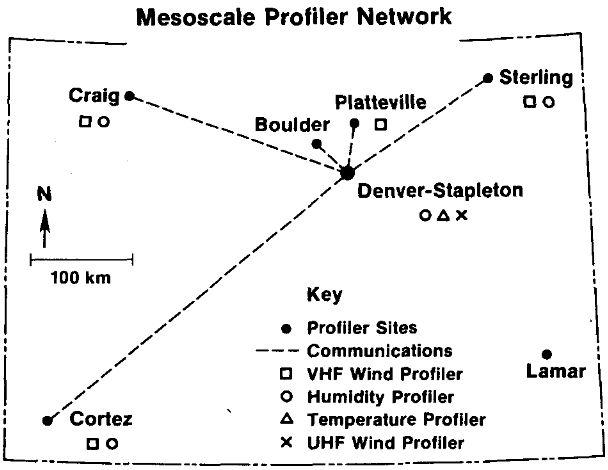


FIG. 26. Network of three outlying stations in the State of Colorado communicate with the host computer at Denver (long dashed lines); each station will house a VHF radar wind Profiler and a radiometric humidity Profiler to obtain data for research in mesoscale weather forecasting.

will be auto-dialed every hour by the host computer at Denver (Section 8) for processing and distribution of data to the users.

It is believed that provisions of hourly profiles of humidity and wind will be meaningful to research and operations meteorologists interested in the flux of water vapor into and out of the region, and for improved prediction of weather for the city of Denver and its environs. The influence of the mountain range, and the prediction of orographic precipitation and severe downslope (chinook) wind storms will also be investigated.

### *e. Profiler for weather service operations*

The remote-sensing system discussed in the previous sections is a prototype. Although its capability is fully exercised in providing continuous data sets for research in weather forecasting, some of the subsystems are not of optimum design for an operational Profiler for the weather services. For instance, only one of the remote-sensing subsystems (the 20.6/31.6 GHz radiometer, Section 5) is at present being produced by a major manufacturer. The algorithms for real-time implementation of active/passive profiling, adaptive coefficients, and combined satellite/Profiler profiles (all discussed in the previous sections) have yet to be realized.

It is clear that the wind-profiling function, provided by two Doppler radars in the prototype, must be accomplished by a single instrument in an operational Profiler. The physics that governs the operating frequency of a radar that can profile the boundary layer with adequate resolution in altitude, and also provide information on tropopause heights, is discussed in Section 6. In all likelihood, a frequency in the upper VHF or lower UHF (i.e., ~300 MHz) would be suitable. A development such as this is not undertaken lightly since matters such as frequency allocation, economics and electronic design must be considered in addition to the electromagnetic behavior of the atmosphere. The operational aspects of wind profiling have also been discussed by Larsen and Röttger (1982) and by Balsley and Gage (1982).

As discussed in Section 7, an automatic instrument for measurement of the height of a cloud base would provide a valuable input for improvement of humidity profiles. At present, the weather services are considering new designs of ceilometers, based primarily on near-infrared lidar techniques. It is possible, however, that Doppler millimeter-wave radar with fixed, vertically pointing antenna beam and solid-state components may become competitive.

The data system of the Profiler, outlined in Section 8, at present consists of a host computer along with special data processors associated with individual instruments. In the operational design, it is planned, by way of efficiency and economy, to have almost all functions performed by a single computer. The required capacity of that computer will not, however, be definable until all of the algorithms are implemented and proven. In any case, the capacity required of the computer will be minimized for operational application.

It is planned that the operational Profiler be implemented in close collaboration with the weather services to ensure that compatibility with existing hardware and software, such as the AFOS system and the satellite systems, is achieved.

*Acknowledgments.* Many people and organizations are contributing to implementation of the Profiler: the Aeronomy Laboratory of ERL/NOAA cooperates in both the design and operation; the WSFO of the National Weather Service, Stapleton Airport, Denver, provides a site and meteorological data; the National Meteorological Center, the National Environmental Satellite Service, the University of Wisconsin and the National Climatic Center of NOAA provide consultation and data. In particular, we thank C. E. Case, V. Y. Boyle, and J. B. Snider of the Wave Propagation Laboratory for their ongoing contribution, J. M. Fritch, M. E. Pautz, and T. W. Schlatter of the Pennsylvania State University, National Weather Service (NWS), and PROFS Program Office of ERL, respectively, for their help in choosing locations for stations of the Mesoscale Profiler Network, W. E. Hoehne, and R. Stone of the Test and Evaluation Division of NWS for their cooperation and M. A. Shapiro and E. E. Gossard for critical readings of the manuscript.

## REFERENCES

Atlas, D., C. Srivastava and R. S. Sekhon, 1973: Doppler radar characteristics of precipitation at vertical incidence. *Rev. Geophys. Space Phys.*, **2**, 1–35.

Balsley, B. B., and W. L. Ecklund, 1972: A portable coaxial colinear antenna. *IEEE Trans. Antennas Propag.*, **AP-20,** 513–516.
——, and K. S. Gage, 1982: On the use of radars for operational wind profiling. *Bull. Amer. Meteor. Soc.*, **63,** 1009–1018.
Browning, K. A., and R. Wexler, 1968: A determination of kinematic properties of a wind field using Doppler radar. *J. Appl. Meteor.*, **7,** 105–113.
Chadwick, R. B., K. P. Moran, R. G. Strauch, G. E. Morrison and W. C. Campbell, 1976: Microwave radar wind measurements in the clear air. *Radio Sci.*, **11,** 795–802.
Decker, M. T., 1978: Microwave radiometer studies in PHOENIX. *Project PHOENIX,* NOAA/NCAR-Boulder Atmospheric Observatory Rep. No. 1, W. H. Hooke, Ed., 69–79.
——, E. R. Westwater and F. O. Guiraud, 1978: Experimental evaluation of ground-based microwave radiometric sensing of atmospheric temperature and water vapor profiles. *J. Appl. Meteor.*, **17,** 1788–1795.
Earnshaw, K. B., D. C. Hogg and R. G. Strauch, 1983: A triple-beam antenna for a wind-profiling radar. Submitted for publication in *IEEE Trans. Antennas Propag.*
Ecklund, W. L., D. A. Carter and B. B. Balsley, 1979: Continuous measurement of upper atmospheric winds and turbulence using a VHF Doppler radar: Preliminary results. *J. Atmos. Terr. Phys.*, **41,** 983–994.
——, K. S. Gage, B. B. Balsley, R. G. Strauch and J. L. Green, 1982: Vertical wind variability observed by VHF radar in the lee of the Colorado Rockies. *Mon. Wea. Rev.*, **110,** 1451–1457.
Fischler, M. A., and R. C. Bolles, 1981: Random sample consensus: A parodigm for model fitting with applications to image analysis and automated cartography. *Commun. Assoc. Comput. Mach.*, **24,** 381–395.
Gage, K. S., and B. B. Balsley, 1978: Doppler radar probing of the clear atmosphere. *Bull. Amer. Meteor. Soc.*, **59,** 1074–1093.
——, and J. L. Green, 1979: Tropopause detection of partial specular reflection with very-high-frequency radar. *Science,* **203,** 1238–1240.
Gossard, E. E., D. R. Jensen and J. H. Richter, 1971: An analytical study of tropospheric structure as seen by high-resolution radar. *J. Atmos. Sci.*, **28,** 794–807.
Guiraud, F. O., J. Howard and D. C. Hogg, 1979: A dual-channel microwave radiometer for measurement of precipitable water vapor and liquid. *IEEE Trans. Geosci. Electron.*, **GE-17,** 129–136.
Hoehne, W. E., 1980: Precision of National Weather Service upper-air measurements. NOAA Tech. Memo. NWS T&ED-16.
Hogg, D. C., and T. S. Chu, 1975: The role of rain in satellite communications. *Proc. IEEE,* **63,** 1308–1331.
——, F. O. Guiraud, C. G. Little, R. G. Strauch, M. T. Decker and E. R. Westwater, 1980a: Design of a ground-based remote sensing system using radio wavelengths to profile lower atmospheric winds, temperature, and humidity. *Remote Sensing of Atmospheres and Oceans,* Vol. 14, A. Deepak, Ed., Academic Press, 313–364.
——, —— and E. B. Burton, 1980b: Simultaneous observation of cool cloud liquid by ground-based microwave radiometry and icing of aircraft. *J. Appl. Meteor.*, **19,** 893–895.
——, —— and W. B. Sweezy, 1981: The short term temporal spectrum of precipitable water vapor. *Science,* **213,** 1112–1113.
——, ——, J. B. Snider, M. T. Decker and E. R. Westwater, 1983: A steerable dual-channel microwave radiometer for measurement of water vapor at liquid in the troposphere. *J. Climate Appl. Meteor.*, **22,** 789–806.
Kolmogorov, A. N., 1941: Interpolation and extrapolation von stationaren zufalligen folgen. *Bull. Acad. Sci. USSR, Ser. Math.*, **5,** 3–14.
Larsen, M. F., and J. Röttger, 1982: VHF and UHF radars as tools for synoptic research. *Bull. Amer. Meteor. Soc.*, **63,** 996–1008.
Röttger, J., 1980: Reflection and scattering of VHF radar signals from atmospheric refractivity structures. *Radio Sci.*, **15,** 259–276.
Smith, W. L., T. W. Nagle, C. M. Hayden and H. M. Woolf, 1981: Vertical mass and moisture structure from TIROS-N. *Bull. Amer. Meteor. Soc.*, **62,** 388–393.
Strauch, R. G., 1981: Radar measurement of tropospheric wind profiles. *Preprints 20th Conf. Radio Meteorology,* Boston, Amer. Meteor. Soc., 430–434.
Westwater, E. R., 1967: An analysis of the correction of range errors due to atmospheric refraction by microwave radiometric techniques. ESSA Tech. Rep. IER 30-ITSA 30.
——, 1972: Ground-based determination of low altitude temperature profiles by microwaves. *Mon. Wea. Rev.*, **100,** 15–28.
——, 1978: The accuracy of water vapor and cloud liquid determination by dual frequency ground-based microwave radiometry. *Radio Sci.*, **13,** 677–685.
——, and O. N. Strand, 1968: Statistical information content of radiation measurements used in indirect sensing. *J. Atmos. Sci.*, **25,** 750–758.
——, and N. C. Grody, 1980: Combined surface- and satellite-based microwave temperature profile retrieval. *J. Appl. Meteor.*, **19,** 1438–1444.
——, and F. O. Guiraud, 1980: Ground-based microwave radiometric retrieval of precipitable water vapor in the presence of clouds with high liquid content. *Radio Sci.*, **15,** 947–957.
——, M. T. Decker, A. Zachs and K. S. Gage, 1983: Ground-based remote sensing of temperature profiles by a combination of microwave radiometry and radar. *J. Climate Appl. Meteor.*, **22,** 126–133.
Wiener, N., 1949: *Extrapolation, Interpolation, and Smoothing of Stationary Time Series.* Wiley, 163 pp. [see Chap. 2]